The International Journal of Advanced Manufacturing Technology (2020) 106:2079–2099
https://doi.org/10.1007/s00170-019-04682-2

ORIGINAL ARTICLE

Supersonic particle deposition as an additive technology: methods, challenges, and applications

Zachary Monette[1] · Ashish K. Kasar[1] · M. Daroonparvar[2,3] · Pradeep L. Menezes[1]

Received: 13 July 2019 / Accepted: 10 November 2019 / Published online: 16 December 2019

Abstract
This paper presents a review of recent research inventions in the field of supersonic particle deposition (SPD) additive manufacturing (AM) technology. The SPD, also known as cold spray, is a coating technique that has gained popularity recently because of its ability to apply multi-component coatings. The SPD has the potential to revolutionize the global parts manufacturing and logistics landscape. The state-of-the-art, rapidly emerging cold spray manufacturing technology is an alternative to traditional additive manufacturing (AM) based on powder melting. It enables the rapid fabrication of parts that have properties similar to the parts developed by conventional manufacturing. In this paper, the history and process of SPD are explained. A broad background of metallic SPD AM is provided. SPD parameters, including substrate and particle properties, are discussed. Common challenges in creating consistent SPD coatings as well as challenges specific to metal and ceramic SPD are discussed. This paper explores the material science, processes, and performance gain. Several applications of SPD, including nuclear, aerospace, and electrical industries, are discussed.

Keywords Cold spray coating · Additive manufacturing · Composite coating · Peening · Supersonic particle deposition

1 Introduction

Coatings are used to protect the substrate and improve properties, such as wear resistance, electrical conductivity, anti-corrosion, etc., using suitable materials. Coatings can also be inexpensive. Multifunctional materials can be coated with a high-performance coating, which can improve the life of the component without much increase in cost. There are many different methods to apply coatings, some of which include electrodeposition, supersonic particle deposition (SPD), physical vapor deposition (PVD), chemical vapor deposition (CVD), submersion, and sputtering.

Supersonic particle deposition (SPD) is an effective method of creating coatings through the application of multiple layers of sprayed particles deposited on the substrate. The SPD process was discovered by chance in the 1980s in Siberia. Small particles were added to a wind tunnel containing a substrate, to study the erosive effect. The researchers noticed that when spray particles reached a critical velocity, the particle adhered to the substrate without eroding it [1, 2]. SPD is also called cold spray, cold gas spray, micro cold spray, cold gas dynamic spray, kinetic spray, or metal powder application [3]. Recently, the SPD technique has gained popularity because of its ability to apply multi-component coatings [4]. Currently, the most common use of the SPD technique is applying a metallic or composite coating to a metal substrate.

SPD is a solid-state process because it is performed at a temperature below the melting point of the spray particle (feedstock) materials, making it suitable for temperature-sensitive materials like polymers and nanocrystalline material. SPD's solid-state process is also advantageous for materials that oxidize quickly, such as aluminum (Al) and copper (Cu), unlike traditional thermal spray methods [5]. During the SPD process, the powder particles are deformed in just a few nanoseconds [6] as built-up kinetic energy is converted to heat that cannot be conducted away from the contact area when the

✉ Pradeep L. Menezes
pmenezes@unr.edu

[1] Department of Mechanical Engineering, University of Nevada, Reno, NV 89501, USA

[2] Research and Development Department, ASB Industries, Inc., Barberton, OH 44203, USA

[3] Department of Chemical and Materials Engineering, University of Nevada, Reno, NV 89501, USA

spray powder particles are striking the substrate. This heat forces both the substrate and spray powder to recrystallize and limits strain hardening. The interface of the substrate and the spray powder particle is a type of solid-state welding [6]. Figure 1 shows a schematic of a typical SPD setup. It shows that pressurized gas is used to propel powders to make a solid-state coating.

SPD technique can be classified into two types: low-pressure and high-pressure. Low-pressure SPD systems typically operate below 10 bars of pressure, while high-pressure sprayers can operate up to 40 bars [7]. Low-pressure systems require smaller equipment and are more portable, and results in particles being accelerated to velocities between 300 and 600 m/s. High-pressure SPD systems require more machinery, result in higher velocity, and can be used for particles that have a higher density such as nickel, gold, silver, and some metal matrix composites.

The coating fabricated by the SPD technique has many advantages over other coating methods. Other than applying a uniform coating on a substrate, it can also be employed to restore and repair a damaged substrate. SPD can be used to apply coatings only to targeted areas and is more precise than some coating methods, like submersion. The other main advantage of SPD is working temperature because it does not require heating the coating material to make it bond to the substrate, like PVD and other methods requirements. SPD has less waste compared to other methods. Also, SPD machinery can be portable, enabling coatings to be applied outside of a laboratory setting. SPD can also be applied using non-conductive materials and other mixed composites, unlike electrodeposition.

Current research has been focusing on experimenting with diverse components in the SPD powder and various parameters in the SPD method to produce coatings that can alter the characteristics and performance of the substrate. In this paper, we review various SPD methods and their parameters, different SPD materials, and their effect on the substrate characteristics and performance. The challenges during the SPD are also discussed, followed by the application of SPD coatings in various fields, such as automotive, aerospace, and nuclear.

2 SPD parameters and materials

In SPD coatings, properties of the spray materials and processing parameters impact the outcome. SPD coatings perform very differently based on the spray materials, substrate properties, and processing parameters applied in the process. To achieve the desired results, a thorough understanding of SPD methods, coating materials, and substrate properties are needed.

2.1 SPD parameters

The efficiency of the SPD process is defined by the ratio between the weight of particles that stick to the substrate and the weight of all particles fired. This ratio is also known as deposition efficiency (DE). Higher DE is preferable as it is more efficient and more cost-effective. When firing softer particles at a harder substrate, the DE is largely dependent on the particle plasticity, and this process has been extensively modeled and documented. In contrast, when hard particles are fired at a relatively softer substrate, the DE depends on the mechanical interlocking and physical trapping, especially for the first layer [8]. The DE also relies on spray particle's shape, size, impact velocity, and initial temperature.

SPD coatings can be made up of a combination of metals, ceramics, and polymers. Because the different particles will have different critical velocities, and harder metals demand more energy, ideal settings for one particle selection may be ineffective for another. Therefore, such composite coatings require tuning of processing parameters to achieve critical velocities for all the constituents and yield uniform coatings [4]. An understanding of the characteristics of each component of the spray mix is required for predictable results. Various SPD methods, their

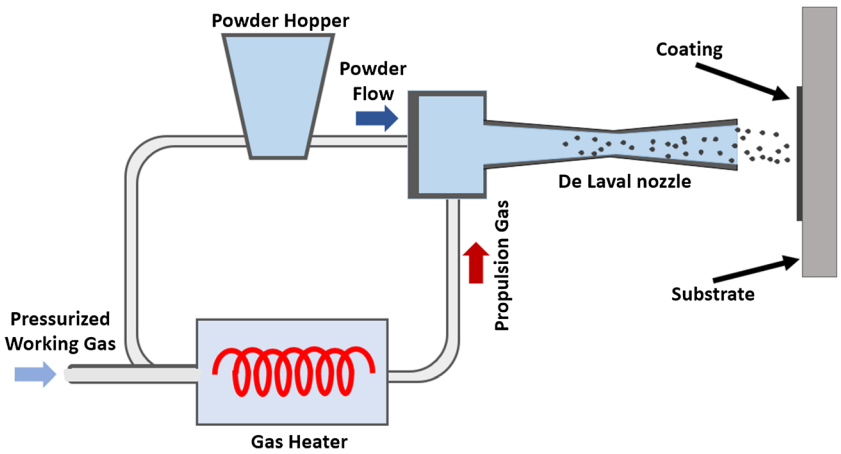

Fig. 1 Schematic of the SPD setup. Pressurized working gas propels powders to create a solid-state coating

parameters, and the resulting coatings deposition efficiency are discussed below.

2.1.1 Velocity, impact, and deformity

The velocity of SPD particles affects the impact on the substrate and the deformity of the spray particles, thus affecting the quality of the coating. SPD particles can reach velocities ranging from 200 to 1400 m/s. The choice of process gas used in SPD significantly affects the spray particle velocity. Low-pressure SPD systems typically utilize air or nitrogen for the process gas. Compressed air is used when a lower range of velocity is acceptable. Nitrogen is used in low-pressure systems when higher velocity is required. High-pressure SPD particles are typically accelerated to velocities between 800 and 1400 m/s [9] using helium or nitrogen for the process gas. The velocity ranges for high- and low-pressure SPD are presented in Table 1. Helium will result in higher velocity than nitrogen, but it is more expensive. The high-pressure SPD process results in a higher coating density than low-pressure SPD process. Low-pressure SPD is cheaper than high-pressure SPD because of equipment and processing gas.

Metal and metal composite coatings possess higher hardness properties due to the immense strain hardening that the particles undergo. For example, stainless steel powder demonstrates a Vickers hardness number of HV180 ± 45. The resultant coating, created via SPD at a high temperature (600 °C) and high gas pressure (40 bar), showed a 100% increase in hardness HV358 ± 36 [10]. Table 2 shows changes in pressure and temperature that resulted in different hardness values.

As hardness increases, there is a tradeoff in reduced ductility. The strain hardening can be a benefit or a liability, for instance with the stainless-steel coating mentioned above, the strain hardening results in a reduction in ductility, with some stainless-steel-coated samples reaching as low as 0% strain, although a portion of the ductility can be restored via heat treatment.

Generally, higher particle velocity results in higher deposition efficiency and coating density [11] because spray particle velocity affects the impact pressure on the substrate, which in turn affects the amount of shear stress both the substrate and the coating materials undergo. Figure 2 shows the relationship between impact velocity and impact pressure for 15 μm pure Al particles sprayed on a ZE41A Mg alloy substrate. The impact pressure is calculated using the linear momentum transfer over the impact time. As velocity increases, impact pressure also increases.

Using velocities that are too low will result in no adhesion; however, using velocity that is too high will result in substrate erosion. Dean et al. [13] explained that the critical velocity is the lowest velocity in which a particle will adhere to the substrate, and the erosion velocity is the velocity at which the particle no longer adheres, but instead erodes the substrate.

Table 1 Velocity ranges for low- and high-pressure SPD

System type	Gas	Velocity range
Low pressure	Compressed air or nitrogen	200–800
High pressure	Nitrogen or helium	800–1400

For example, copper starts to bond to low carbon steel around 350 m/s, though the bond is weak. At 600–750 m/s, the bond is better, but at impacts beyond this velocity, there is significant substrate material loss. At 1150 m/s, there is no longer any deposition, and when the impact velocity is more than 1450 m/s, there is only erosion [14]. Moridi et al. [15] explain that the critical velocity and the erosion velocity are more dependent on the particle material and less dependent on the substrate choice. The effect of a copper spray coating applied at different velocities to a low carbon steel substrate surface is shown in Fig. 3. It shows that bonding starts to occur around 350 m/s, and that optimal bonding is achieved between 600 and 750 m/s. At velocities higher than 750 m/s, erosion begins to occur. At velocities higher than 1000 m/s, adhesion no longer takes place, and at 1450 m/s, erosion results in substantial material loss.

Table 3 shows the critical velocity, erosion velocity, and the melting point of popular SPD powder materials. A general trend can be seen that the materials with higher melting points have higher critical velocity. For composite spray particle powders, due to various size distributions, it is entirely possible that some particles will be below critical velocity, and some will be above erosion velocity while most of the particles are right in the desired velocity range [13].

Typically, higher particle velocity is associated with greater deposition efficiency. However, Jenkins et al. [17] suggested that particle velocity does not always constitute a higher coating density. During the SPD process, subsequent layers compress previously sprayed layers as new particles strike the sprayed coating. This is known as tamping, and tamping usually strengthens the bond between the substrate and the coating layers. Tamping causes strain to the spray particles, resulting in a cold weld between the substrate and the spray

Table 2 Hardness values of sprayed stainless steel particles [10]

Gas temperature [°C]	Gas pressure (bar)	Hardness (HVN)
600	20	338 ± 44
	30	340 ± 66
	40	358 ± 36
700	20	353 ± 72
	30	314 ± 58
	40	333 ± 57
800	20	310 ± 61

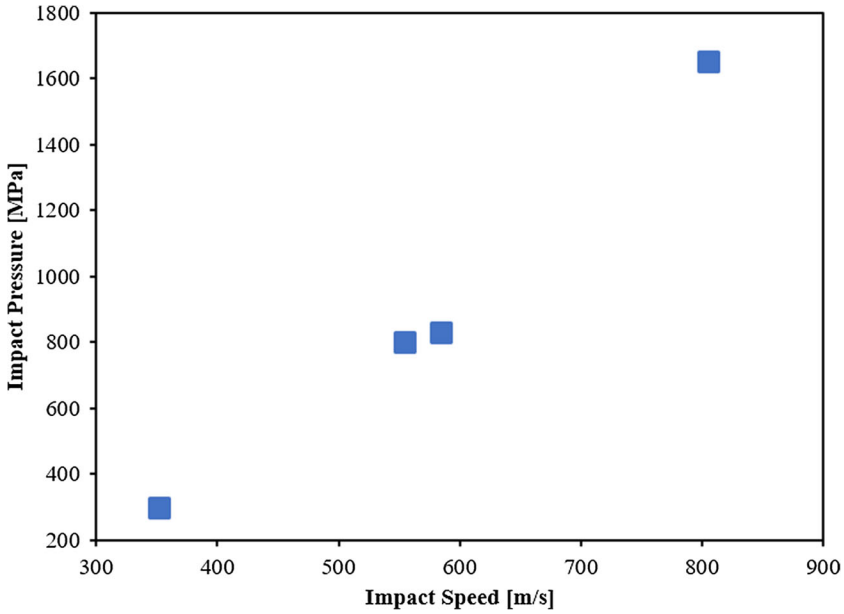

Fig. 2 Impact velocity versus impact pressure for 15 μm pure Al particles sprayed on a ZE41A Mg alloy substrate [12]

particles. The cold weld is essential for optimal bond strength. There can be negative effects of tamping, however, depending on the coating particles used. For example, aluminum spray particles experience an inverse relationship of velocity to coating density due to tamping. The strain hardening of the lower layers makes it harder for subsequent layers to adhere. Jenkins et al. [17] recommend attaining a balance between velocity and coating density and mitigating the negative effects of tamping on certain materials. Similar behavior has been observed by Xiong [18] using nickel and aluminum.

Deformity refers to the effect of impact on both the particles and the substrate. When the sprayed particles impact the substrate, both the particles and the substrate are deformed. For example, Fig. 4 shows the scanning electron microscope (SEM) and optical images of WC-12Co coated on aluminum alloy by SPD where both the coating and the substrate are

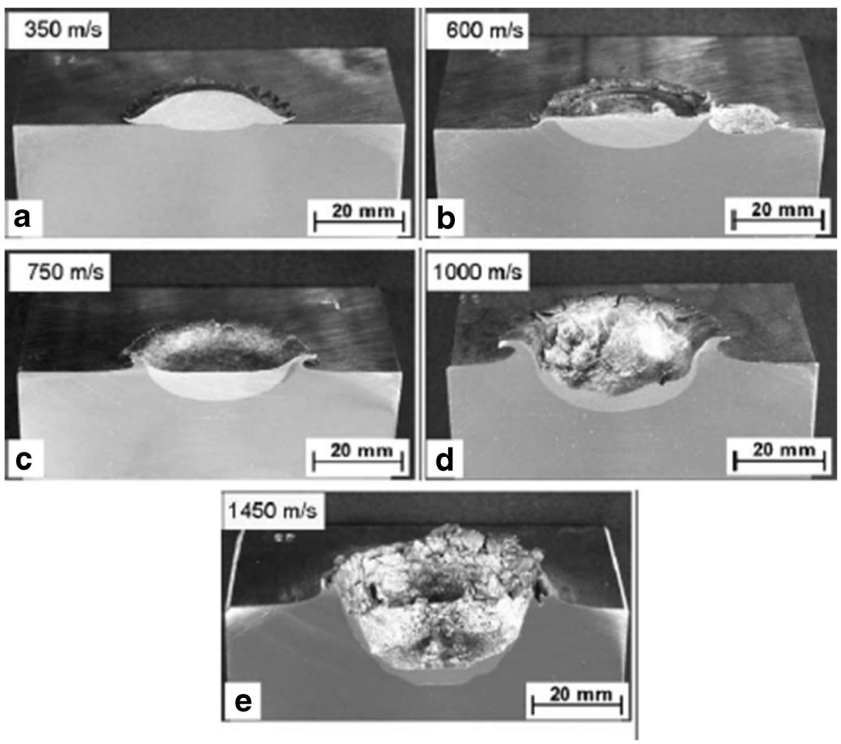

Fig. 3 Impact of the copper sphere against low carbon steel at different particle velocities. Bonding starts to occur at around 350 m/s (**a**). Optimal bonding is achieved between 600 and 750 m/s (**b**, **c**). At velocities higher than 750 m/s, erosion begins to occur. At velocities higher than 1000 m/s, adhesion no longer takes place (**d**). At 1450 m/s, erosion results in a substantial material loss (**e**) [14]

Table 3 Material properties of popular SPD powder materials [3, 14, 16]

Spray material	Melting point [°C]	Critical velocity [m/s]	Erosion velocity [m/s]
Tin	232	160	320
Zinc	420	339	700
Magnesium	650	607	1560
Aluminum	660	482	1250
Copper	1084	451	930
Steel 316L	1400	655	1375
Nickel	1455	574	1200
Iron	1538	596	1300
Titanium	1670	712	1375

deformed. The substrate deforms plastically and forms intermetallic bonds with the spray particles. Due to plastic deformation, extruded lips can also be seen in Fig. 4a. Spencer et al. [12] studied aluminum particles sprayed on magnesium substrate and found that the bond strength also resulting from the residual compressive stress introduced during impact when particles strike the substrate. This localized compressive stress strengthens the substrate and coating. When aluminum particles are sprayed with a nozzle temperature of 217 °C and 400 °C, the residual stress decreased from − 21 to − 35 MPa. This could be due to material softening, or higher pressure, which occurs as a result of the increased nozzle temperature [12].

2.1.2 Impact angle

The impact angle of the spray particles can affect the quality of the coating. Wang et al. [19] describe that the bonding strength of SPD coating with the substrate is dependent on the spray angle and that the bond strength increases as the spray angle is decreased from 90° to 45°. However, the deposition efficiency and the strength of the spray coating decreased with a decrease in spray angle. Also, as the spray angle is decreased, the bond starts to create gaps, and the penetration of the particle is lessened, as shown in Fig. 5.

2.1.3 Pre-processing of spray particles

The particle size of the spray particles has an impact on the finished microstructure of the coating. Brewer et al. [11] suggest that SPD powders that are previously cold-worked or carrying high dislocation density can enhance the grain quality of the coating. Grain refinement can be achieved by cryomilling and ball-milling of SPD particles. Research shows that grain refinement of SPD particles has been used to achieve fully nanocrystalline coatings in aluminum [20], copper [21], iron [22], and nickel [23], thus controlling the effects of particle size on the results.

Grain refinement is of particular importance because the grain size of the powder influences the performance of the coating. When the particle size is small, uncertainty in velocities from wide spray particle distribution is reduced. Because the spray particles are closer in size to each other, they will perform in similar ways. Smaller spray particles are also typically associated with higher coating density. The smaller particles can fill in the gaps in the previously sprayed coating layer. Rokni et al. [24] explain that smaller grains lead to harder coatings because the particles experience more strain hardening and strengthening from subsequent sprayed layers. SPD coating methods and parameters are varied and can make attaining predictable results difficult. Continued research on the many SPD parameters is needed.

2.2 Spray particle materials

SPD can be used with a wide variety of particle materials, including ceramics, metals, polymers, and composite materials. Each material has unique characteristics and possible applications. Table 4 shows common spray particle materials used for the SPD with their associated benefits and potential applications.

Many traditional benefits of material coatings can be achieved with SPD, including inhibiting corrosion, reducing friction, and wear, making biocompatible coatings. Metal and metal-composite SPD materials are used for many applications because of their unique properties. For example, metal

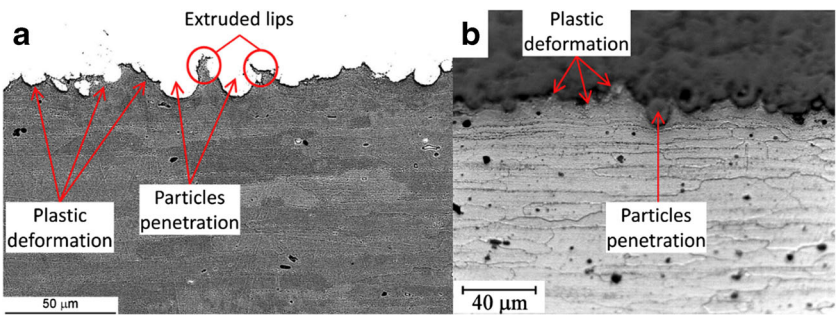

Fig. 4 **a** SEM and **b** optical micrograph showing the etched cross-section of aluminum alloy substrate with WC-12Co coating shows plastic deformation on the substrate as well as coating particle [6]

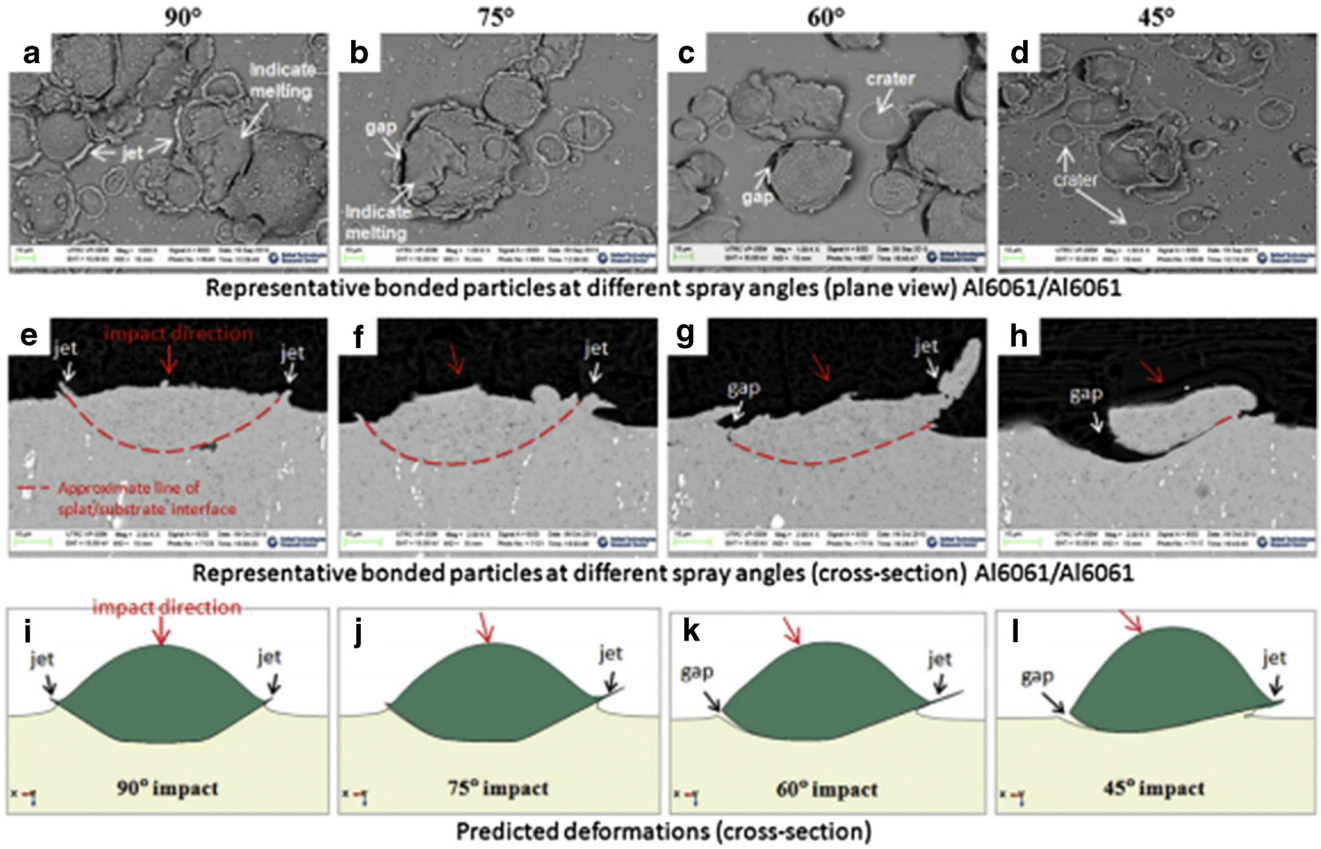

Fig. 5 Effect of the spray angle on bonding depth between Al6061/Al6061. Spray angle 90° (**a**, **e**, **i**). Spray angle 75° (**b**, **f**, **j**). Spray angle 60° (**c**, **g**, **k**). Spray angle 45° (d), (h), (l). Gaps begin to form as the angle is decreased from 90°. Gaps are most pronounced at 45°. Gaps decrease intermetallic bonding between spray particles and substrate and reduce bond efficiency [19]

or metal-composite SPD materials can tolerate higher velocities than ceramic materials, and therefore typically have a higher deposition efficiency. Two common SPD materials, aluminum and titanium, are discussed below with processing parameters.

Aluminum composite spray coatings have been developed and tested and are becoming valuable in marine, nuclear, military, and similar fields. These composite coatings have a high specific strength, good thermal stability, good wear resistance, and superior seizure resistance. Ceramic particles can be

Table 4 Common materials used for SPD, their benefit, and their potential applications [9, 11, 13, 25–30]

Spray particle material	Benefit	Application
Cu, Ag	Increased conductivity, no oxidation, higher material homogeneity	Electronics, protection from corrosion, heat transfer
Al, Mg alloys	Good bonding, similar strength to bulk material	Component repair
Al, Ti alloys	Manufactured components with few interface defects, corrosion resistance	Additive manufacturing, tribological spray, marine applications
Cu alloys	Reduce friction/wear, self-lubricating composite components	Tribological coating
Ti alloys	Biocompatibility	Biomedical components
Steel (ferritic austenitic)	Magnetic, comparable strength to bulk material, corrosion resistance	Component repair, biomedical SPD tamping for softer SPD particles
Ni alloys	Hot gas resistance, energetic material coatings	Aerospace, component repair
Carbon nanotubes	Increase thermal and electrical conductivity	Electronics, heat sinks
WC (tungsten carbide)	Wear resistance	Industrial components
B_4C composites	Neutron shielding	Nuclear, aerospace, military

Table 5 SPD parameters for aluminum

Gas temp [°C]	Gas pressure [MPa]	Particle dize [μm]	Impact velocity [m/s]	Gas	Ref
450	5.7	15–63	–	Nitrogen	[31]
450	2.7	25	620	Nitrogen	[32]
250	3.0	–	–	Nitrogen	[33]
450	2.5	2–12 15–45	–	Nitrogen	[34]
132	0.62	15	585	Helium	[12]
217	0.76	15	352	Nitrogen	
550	3.85	15	805	Nitrogen	
400	3.85	45	615	Nitrogen	

added to enhance these properties further. The parameters for applying aluminum composite coatings by SPD, including gas temp and gas pressure, are presented in Table 5.

Lek et al. [35] explained that titanium is highly favorable for many applications, including biomedical implants. Because the raw materials are expensive, the SPD could be used to repair damaged components instead of replacing them. The SPD process results in a compact coating with a high deposition rate, high dimensional tolerance, and minimal heat-affected zones. This allows the microstructure of the feedstock to be preserved and minimizes the effects of high-temperature damage to the substrate and the feedstock [35]. Table 6 presents the SPD parameters for using titanium as a spray particle (feedstock) including working gas type, pressure, and temperature.

2.3 Substrate Properties

The performance of the SPD coatings does not only depend on the spray particle properties but also on the substrate properties [38]. The properties of the substrate will affect how well the SPD layers interact with the substrate and with each other. Properties of the substrate can affect the deposition of the first layer of the spray coating, thus affecting all the successive layers.

There are two important types of interactions in SPD—(a) the interaction between the substrate and the first coating layer and (b) the interaction between the first coating layer and subsequent layers. Because these two interactions are different, it is possible that the requirements for adhesion for each is different. For example, the required velocity could be different depending on the layer. Understanding these interactions is critical to obtaining a successful coating outcome. The first spray coating layer is especially crucial for the adhesive strength of the coating, while the subsequent spray coating layers are essential for the cohesion strength of the coating.

The substrate properties affect not only the first layer but also the properties of the coating as a whole. The harder the substrate, the more severe the deformation of the impacting particle. Softer substrates can experience better bonding because the impact causes adiabatic shear instability on the substrate as well. The substrate temperature at the time of impact can significantly affect the coating quality; even coating particles that are millimeters away from the substrate can be affected by the substrate temperature. The increased substrate temperature is associated with increased areas that were highly strained, thus

Table 6 SPD parameters for titanium feedstock [4, 32, 36–39]

Gas temp [°C]	Gas pressure [MPa]	Impact temperature (particle) [°C]	Particle size [μm]	Impact velocity [m/s]	Gas type	Source
600	1.5	–	25	965	Helium	[32]
600	4.0	–	15	650	Nitrogen	Arabgol et al. (2016)
			34			[38]
			59			
600	3.5	–	23	–	Nitrogen	Sova et al. (2016) [4]
600	3.0	100	5	825	Nitrogen	King et al. (2013)
		380	15	670		[39]
		425	25	600		
		450	35	590		
		425	45	580		
800	3.0	414	12	670	Nitrogen	Faizan-Ur-Rab et al. (2015) [37]
		544	26	500		
		596	41	425		
300	3	–	29	648	Nitrogen	Ajaja et al. (2011)
500	3			723		[36]
800	4			852		

resulting in better bonding. Substrate preheating can improve the quality of SPD coatings up to a millimeter thick [38].

Kumar et al. [32] observed that the roughness of the substrate could also influence the bonding of the sprayed particle. Specifically, the ideal substrate roughness (R_a) is related to the size of the spray particle. The ideal roughness is between 50 and 75% of the particle size, meaning that if the particles are 100 microns, then the R_a for the substrate should be 50–70 microns. This leads to greater bonding from the powder because metallic interlocking can occur. Additionally, substrates that are sandblasted before SPD give more surface area for adhesion and therefore have higher bond rates. In contrast to that, Hussain et al. [40] noted that after grit blasting an aluminum substrate, the substrate had become work-hardened, and the grit particles had become embedded in the substrate surface making it difficult for particles to adhere. Even after annealing to remove the effects of grit-blasted work hardening, the embedded grit particles caused subsequent deposition to be less effective.

2.4 Intermetallic bonding

Xie et al. [41] found that two bonding mechanisms occur in the SPD process: metal-to-metal bonding and mechanical interlocking. Mechanical interlocking is not a chemical reaction; it occurs when hard particles get trapped in softer substrate materials. Metal-to-metal bonding depends on oxide-free particles. Sometimes, as the particle material experiences high strain, a jet of material erupts from the contact surface. It is believed that the oxide is purged through cracks created by the jet. When a single particle is fired at the substrate, the particle impacts and penetrates the substrate. Some interlocking occurs at the rim of the particles, but there is no intermetallic bonding. However, when additional particles are fired, the peening effect cracks the oxide layer, and metal can flow out of the broken cracks, creating metal-to-metal bonding [41]. Xie et al. [41] further explained that due to the "particle peening" or tamping, metal-to-metal bonds exist in SPD with multiple particles (Fig. 6b), but not in single-particle sprays (Fig. 6a). The tamping breaks off the oxide material and allows for a greater metal-to-metal bonding, as shown in Fig. 7.

There are some barriers to inter-metallic bonding. Hussain et al. [40] reported that as oxide layers thicken on the substrate, it is increasingly difficult to form jets during the SPD process, which are necessary for inter-metallic bonding. When inter-metallic bonding is low, the adhesive strength of the coating is controlled by interlocking. Interlocking occurs when substrate material is extruded during the impact. However, when inter-metallic bonds are high, such as in polished or annealed substrates, then the metal-to-metal bonds control the adhesion of the coating.

3 SPD challenges

3.1 Voids

Voids can be a challenge with SPD. King et al. [39] showed that when titanium particles are deposited on a titanium substrate by SPD, voids form in the coating. These voids are a result of inconsistent surface topography. However, 26–77% of these voids are filled in by the plastic flow of the subsequent layer of titanium spray particles due to impact deformation. Upon impact, the particles rapidly convert from kinetic energy to heat through adiabatic shearing, allowing the particle flow to fill in the voids. Lek et al. [35] explained that when impact occurs, a strong shearing force that is typically normal to the impact direction is introduced in the particle near the impact interfaces and provides a driving force that causes adiabatic shear instability to occur.

Voids can be reduced on the titanium substrate by adding larger shot peen materials like stainless steel particles to the titanium spray particles. The large shot peening particles strike the layers of sprayed titanium and compress it further [1]. Figure 8 shows the shot peening effect that can be achieved using SPD when larger particles peen the smaller particles into a smoother coating. Figure 9 shows the size difference between the titanium particles and the stainless-steel particles used to peen the coating.

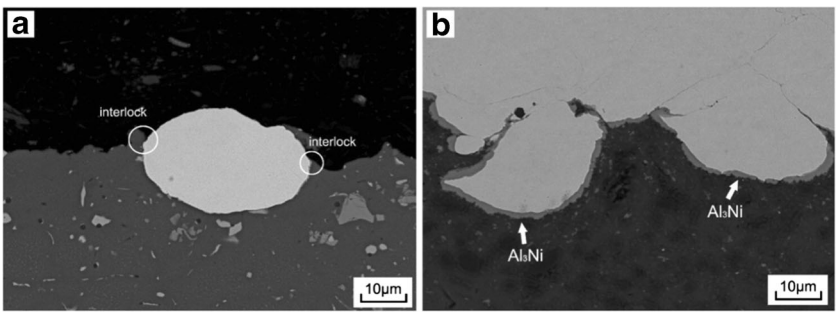

Fig. 6 **a** Single Ni particle by SPD with penetration of substrate and some interlocking at the rim of the particle, but no metallic bonding. **b** Multiple particles by SPD with metallic bonding occurring due to the tamping effect of subsequent layers [41]

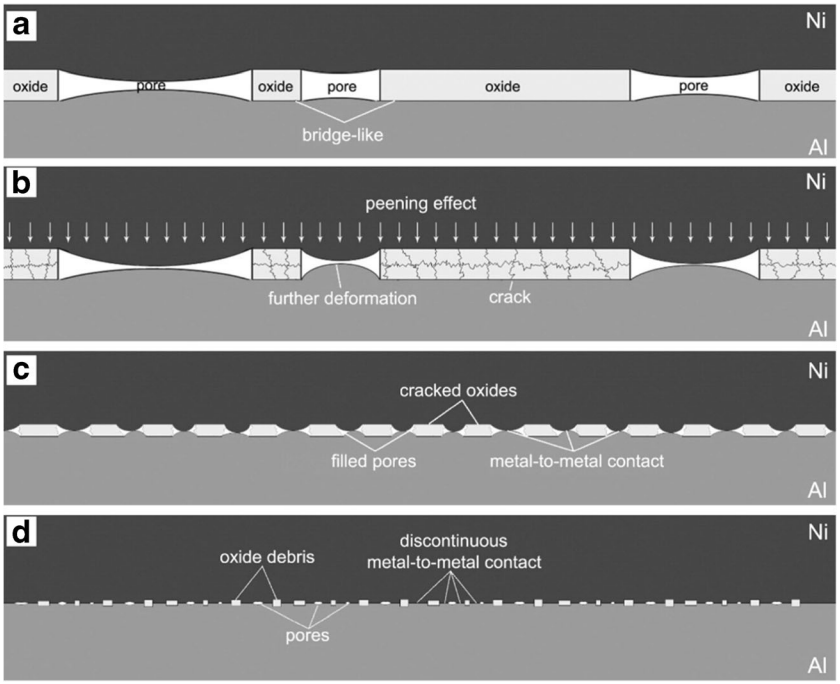

Fig. 7 Schematic of how subsequent particles crack the oxide layers and allow for intermetallic bonding. A single particle layer consists of oxide covered particles and pores where no particles were sprayed (**a**). As subsequent layers are sprayed, they cause a peening effect on the previous layers cracking the oxide layer and deforming the particles (**b**). As the oxide layer cracks, metal can flow out of the cracks creating metal-to-metal bonding (**c**). Metal-to-metal bonding continues as pores are filled in from the metal flow. A portion of oxide debris is blasted away as more particles strike the newly created coating (**d**) [41]

3.2 Challenges during supersonic deposition of metals

Researchers have discovered several problems in the field of SPD that still need solutions. Nikbakht et al. [42] explained that particle bonding remains a point of contention in the research of SPD, especially for asymmetrical pairs, such as Ni and Ti. When a Ni particle is sprayed at a Ti substrate, the particles experience significantly more deformation. However, when a Ti particle is fired at a Ni substrate, both the particle and the substrate experience similar levels of deformation. When both particle and substrate experience similar deformation, the bond of the coating is greatly improved. Because of the rapid strain that occurs, there is insufficient time for heat dissipation, so thermal softening occurs locally and overcomes the strain hardening effect [42].

There has been much research on how to mechanically improve the efficiency of SPD methods. Gärtner et al. [43] suggested that fluid dynamics can be used to design the optimized nozzle geometry [43], while Leitz et al. [44] explained that the initial particle temperature greatly influences the mechanical properties of the coating. The interaction between the particle and the nozzle can be modeled and predicted. Also, the temperature profile of the impacting particle can be simulated to design applications with tailored specifications. At 20 ns, the heat is contained within the zone where the particle struck. The

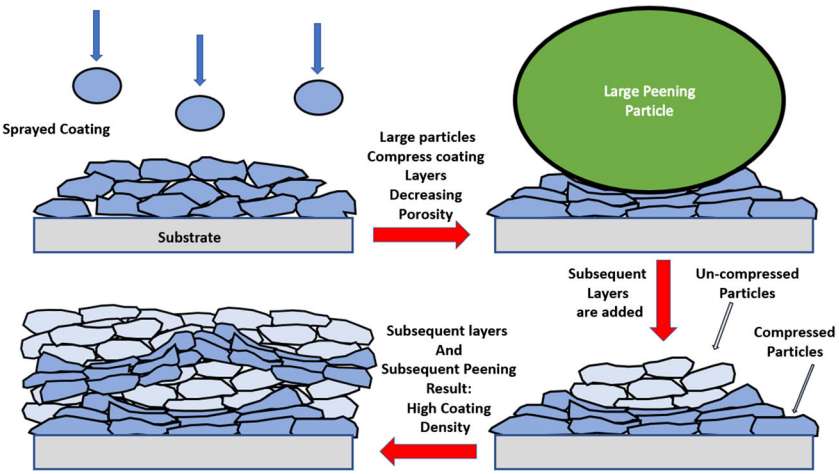

Fig. 8 Schematic of how in-situ shot peening assisted SPD functions

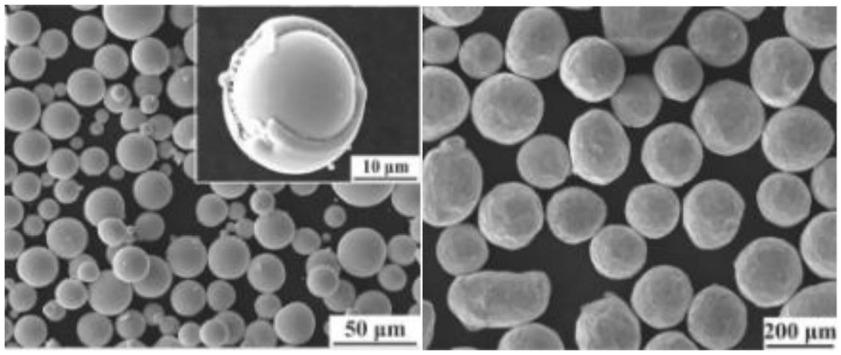

Fig. 9 Titanium particles (left) and stainless steel shot peening particles (right) [1]

heat dissipates through the substrate horizontally reaching the maximum width between 40 and 60 ns. The heat does not reach maximum depth until between 60 and 250 ns [44].

Li et al. [45] stated that the crystal structure of the finished coating could vary. High coating porosity can cause high thermal resistance, unwanted electrical resistance, and poor corrosion resistance. The mix of soft and hard particles for the SPD can be used to obtain fully dense metallic coatings [45].

Winnicki et al. [46] explained that the thicker the coating, the higher the surface roughness. This is because thicker coatings have higher waviness, which forms more extended topography. The bond strength typically holds up to about 61 MPa, depending on the coating thickness. As the sprayed particles strike the substrate, there begins to be some localized heating. As subsequent layers are sprayed, the substrate becomes warmer and softer, leading to differing layer thickness [46].

Malachowska et al. [47] discussed that the spray particle shape and hardness could have a decisive effect on the potential coating formation. Dendrite-shaped powders produce less erosion when sprayed at softer substrates because the contact area between the spray particle and the substrate is greater. Figure 10 shows copper particles for SPD; the micrograph on top shows spherical particles, and the micrograph below presents particles that have a dendrite shape. The dendrite-shaped powders also have more porosity in the final coating.

Softer spray particles are easily deposited on softer substrates, such as lead or tin. When materials like aluminum or titanium are deposited on softer substrates, the SPD process also erodes the substrate. However, when particles like copper are sprayed, the erosion is much more prevalent. Oxidation on the powder can also contribute to poor spray adhesion. The oxygen content can also contribute to poor spray bonding, as the oxide inhibits metallic bonding [47].

Feng et al. [48] discussed that nanoscale twins could improve both strength and ductility, and these twins can limit the movement of dislocations. Nanotwins imply that there is a higher twin density when compared to annealing twins. SPD of copper can create nano twins, and the nano twins create a significant hardening effect of thin coating layers [48].

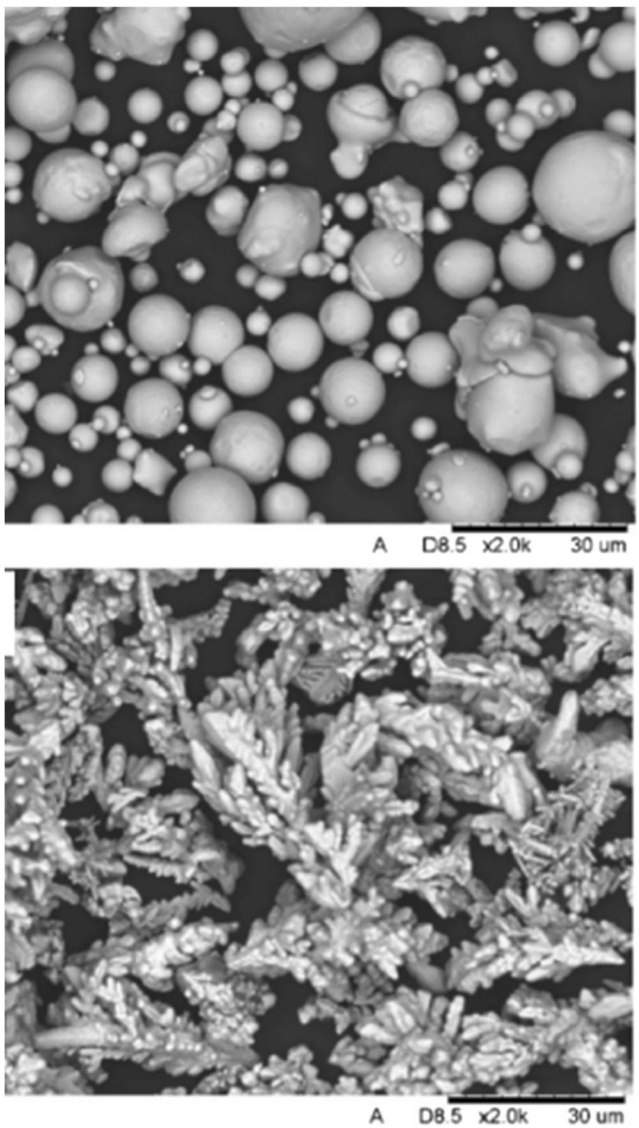

Fig. 10 Spherical copper particles (top) and dendritic copper particles (bottom) used for SPD [47]

3.3 Challenges unique to ceramic and ceramic composites

Dean et al. [13] explained that because ceramic composite spray particle powders have various size distributions, it is entirely possible that some particles will be below the critical velocity, and some will be above erosion velocity while most of the particles are right in the desired velocity range. Lee et al. [49] coated various substrates by boron carbide, titanium carbide, and tungsten carbide using SPD. All three carbides used nickel powder as a matrix, and all three powders had the same SPD parameters applied: compressed air as a carrier gas, and the pressure of 634 kPa at 550 °C. While the SPD parameters were all the same, the tungsten carbide had the highest velocity, twice the boron carbide, and sprayed nearly six times faster than the titanium carbide. Because tungsten carbide had the highest velocity, it experienced more work hardening. To achieve higher deposition rates with the various carbides, the carbide particles need to be significantly smaller than the other material in the composite [49].

Huang et al. [50] coated nickel graphite to aluminum and steel. The authors observed that the graphite particles become more deeply embedded, leaving a distinctly nickel-heavy layer of film coating on the surface for the aluminum substrate. Whereas, even distribution of nickel graphite particles were observed when applied to a steel substrate. When the SPD process was completed, they conducted microhardness tests on the coating of the two substrates, and both showed a hardness of 43 HV, which means that the difference shown in the reaction of the substrate was only applicable to the first layer of the coating.

It can also be expected that the SPD is typically not well suited to materials that will break upon impact, such as ceramics. For example, the coating of ceramic such as SiC on Al can be carried out by co-deposition of Al and SiC. However, it caused the fracture of SiC particulate, as shown in Fig. 11 [51]. To overcome the fracture of ceramic, the quantity of the softer materials in the spray coating mix can be adjusted. These softer materials act as binders. The important criterion to select binding material is the density. Soft materials of similar density to ceramic can provide similar critical velocity and uniform coating. Table 7 shows some common ceramic materials used in SPD coatings and the binders used in conjunction.

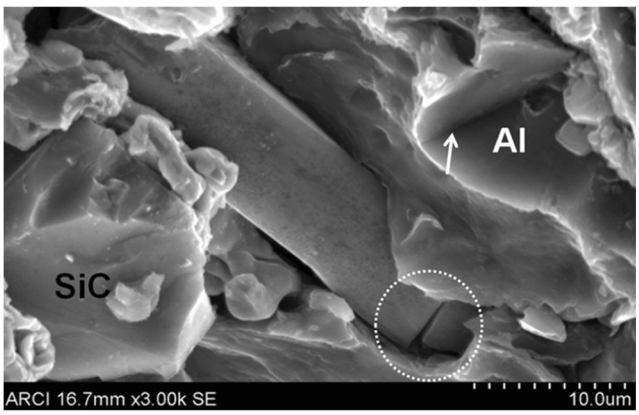

Fig. 11. Fractured SiC particulate from impact (encircled) during the SPD process [51]

Table 7 Common ceramics used in SPD and some typical binding materials (binders)

Ceramic	Binder(s)	Ref
Diamond (nickel coated)	Copper	[52]
Diamond	Aluminum	[53]
Tungsten carbide	Titanium, nickel, aluminum, cobalt	[49, 54–56]
Boron carbide	Nickel, aluminum	[49, 57]
Titanium carbide	Nickel, aluminum	[49, 58]
Aluminum oxide	Aluminum, copper	[55, 59]
Chromium carbide	Aluminum	[55]
Carbon nanotubes	Aluminum-silicon (Al-Si), copper	[26, 60]
Silicon carbide	Aluminum, copper	[59]

4 Applications

SPD coatings have many practical applications in the world today. SPD can be used to increase the life expectancy of sprayed components and can be used to repair components when damaged. Because the SPD is so robust and adaptable, it is well suited to many applications. Some applications are described below.

4.1 Application of SPD in additive manufacturing

Beyond being a coating method, SPD can be used to create components from feedstock powders, acting as an additive manufacturing technique. Assadi et al. [3] described SPD as an alternative to additive manufacturing methods that use selective melting via laser or electron beam. The authors described SPD as a solid-state method for material deposition. It is technically achievable to deposit all metallic and metal-ceramic composites to any thickness beyond 50 μm.

Bagherifard et al. [61] explained that the SPD process could create a coating consisting of a homogeneous microstructure that is similar to the feedstock. This is a contrast to other additive manufacturing techniques, such as selective laser melting (SLM) where the particles undergo dramatic thermal changes. When heat treated, the components fabricated by SPD generate more inter-particle bonding and have remarkable cohesive strength. The heat cycling treatment increases

the ductility and increases the fatigue strength that is comparable to wrought or cast bulk material. At present, heat cycling is a necessary step, as the work hardening of subsequent SPD layers causes the material to be brittle.

An obstacle in the widespread commercialization of SPD as an additive manufacturing process is that the geometrical accuracy is not as tight as with SLM [61]. Components were created using SLM and SPD and their respective properties examined. Both sets of components underwent heat treatment at 1200 °C for 1 h in an argon atmosphere. The components created using SPD showed higher porosity both before and after heat treatment when compared to SLM, as shown in Fig. 12. Figure 13 shows the material properties of these created components, showing that both the SPD and SLM initially produce components that are not as strong as the bulk Inconel material. After heat treatment, both components exceed the standard of the bulk material, with SPD outperforming the laser melting in ultimate tensile strength and yield strength [61]. Heat treatment alleviates the shortcomings of the two additive manufacturing methods.

Yang et al. [62] suggested that SPD is superior as an additive manufacturing process for nonferrous materials because it does not melt the materials, such as copper, aluminum, or magnesium, as laser melt methods do. SPD can be used to create dense parts that exhibit mechanical properties similar to the bulk material, and the SPD process can be scaled up to industrial standards. Yang et al. [62] tested copper samples that were created using SPD. These copper bulk samples were 2 mm thick and 65 mm long. When pulled in tension, the copper bulks broke along grain boundaries of the sprayed material and showed brittle breakage when compared to the annealed sample. The authors also suggested that SPD-created parts should be heat-treated to improve mechanical properties [62].

Although the SPD is considered to be superior to laser melting, Yin et al. [33] have found that combining these two techniques shows promise. Functionally graded materials (FGMs) are materials that have a variety of material microstructures. SPD can be combined with SLM to create these FGMs. Laser melting alone is unsuitable for creating FGMs because when dissimilar materials are welded, they form weak bonds and experience thermal stress. SPD is a desirable choice for "non-weldable" materials. SPD can be used in conjunction with laser melting to produce parts that have different properties. Al + Al_2O_3 were deposited by SPD onto Ti6Al4V components that had been created by SLM. The resulting parts were machinable and had high-quality bonding for the FGM, as shown in Fig. 14. The FGMs were slightly harder than the bulk feedstock due to work hardening during SPD [33].

Jing and Dejun [63] explained how laser re-melting can be used as a post-process on aluminum coatings by SPD. The laser re-melting increases the residual compressive stress of the coating and increases the bond strength. The laser re-melting also increases the electrochemical corrosion resistance and reduces porosity and cracks. The substrate material is diffused below the coating, allowing for greater coating coverage [63].

4.1.1 Oxide-free additive manufacturing process

Luo et al. [25] explained that SPD could be used as an oxide-free additive manufacturing process for metal parts. It can be challenging to obtain dense coating in relatively hard materials such as "Inconel 718 superalloy" when using the cheaper nitrogen gas. However, with the inclusion of bigger stainless-steel particles, the bigger particles hammer the smaller particles, thus forming a denser coating. By including 50% by weight of bigger particles, Inconel coating porosity dropped from 5.6 to 0.26%, resulting in greater inter-particle bonding of the Inconel 718 superalloy as shown in Fig. 15. The coating

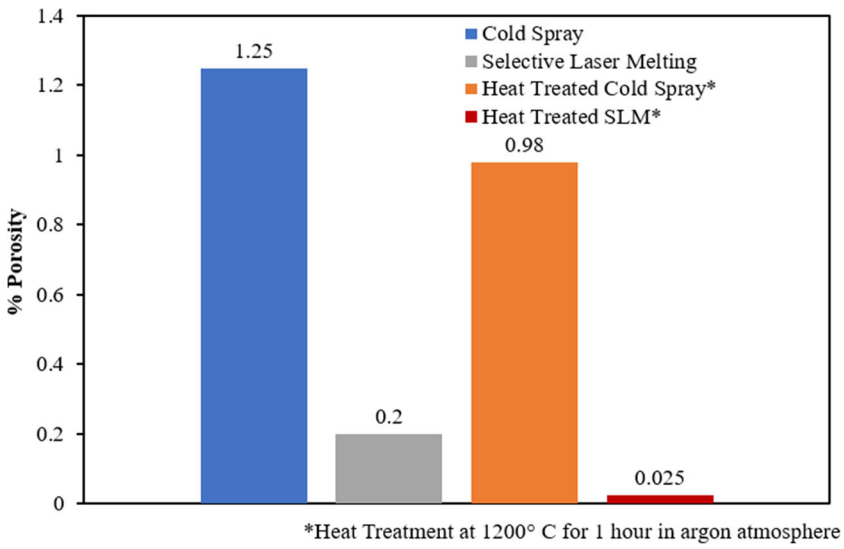

Fig. 12 The porosity of SPD components vs. SLM components both before and after heat treatment. The porosity in SPD components is greater in both cases

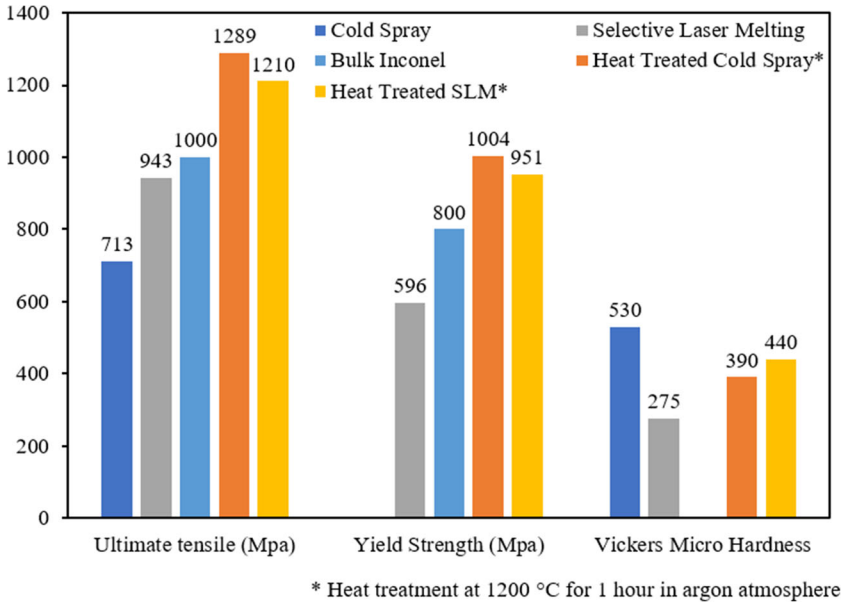

Fig. 13 Material properties of components created via SPD and selective laser melting. Both methods initially create parts that are not as strong as the bulk Inconel material. After heat treatment, both materials are stronger than bulk Inconel

remained uncontaminated because the velocity of the SPD particles was insufficient to embed the larger stainless-steel particles. The reduced porosity also improved the ultimate strength from 96 to 464 MPa.

4.1.2 Industrial case studies on fabrication of 3D components by SPD

Bulk-scale deposition (with high denseness) can be conveniently obtained using SPD technology. Hence, different manufacturing industries are highly interested in additive manufacturing (AM) technology (as component-fabrication method) employing the SPD process. In fact, the SPD method is able to deposit metals, alloys, superalloys, and MMC (metal matrix composites) in bulk scale without any phase transformation, oxidation, and grain growth during the process [64]. Moreover, the SPD process is more affordable than the other current AM processes, such as SLM (selective laser melting) and direct metal deposition. So, several studies have been performed to substantiate the definitive application of the SPD process to AM technology [65–69].

A simple example of a 3D bulk-scale deposit employing SPD additive manufacturing is shown in Fig. 16 [65, 69]. Figure 16 a shows the schematic illustration of SPD aluminum pyramidal fins (near-net-shaped fins) on the metallic bond coated by SPD. It can be seen that 3D fins have been successfully deposited on different metallic bond coatings (Fig. 16b, c). However, some noticeable micro-pores are seen in the coating microstructure. It should be noted that mechanical properties and porosity percentage of SPD deposits could be manipulated using post-spray heat treatments [70]. Other practical examples of symmetrical and intricate components fabrication using SPD or cold spraying additive manufacturing (CSAM) are presented in Figs. 17 and 18. Nevertheless, SPD additive manufacturing of such components is still in the development step and have not been completely commercialized and/or released to the public.

Aluminum (Al) heat exchangers are extensively used in the automotive air conditioning systems. These Al heat exchangers are conventionally produced via intricate production processes, including wire arc spraying Zn layer on Al tubes, cladding fins by dip painting, spreading bond-

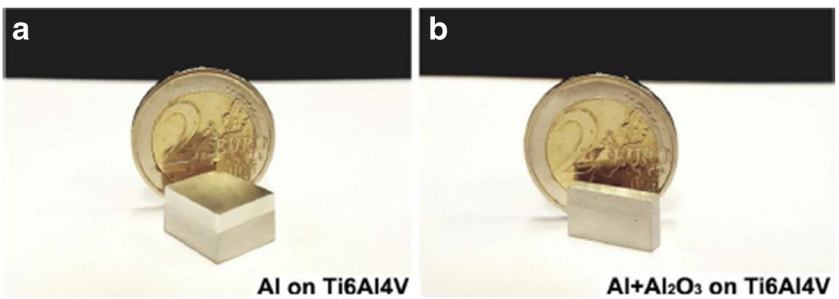

Fig. 14. SPD deposits on selective laser melting created components [33]

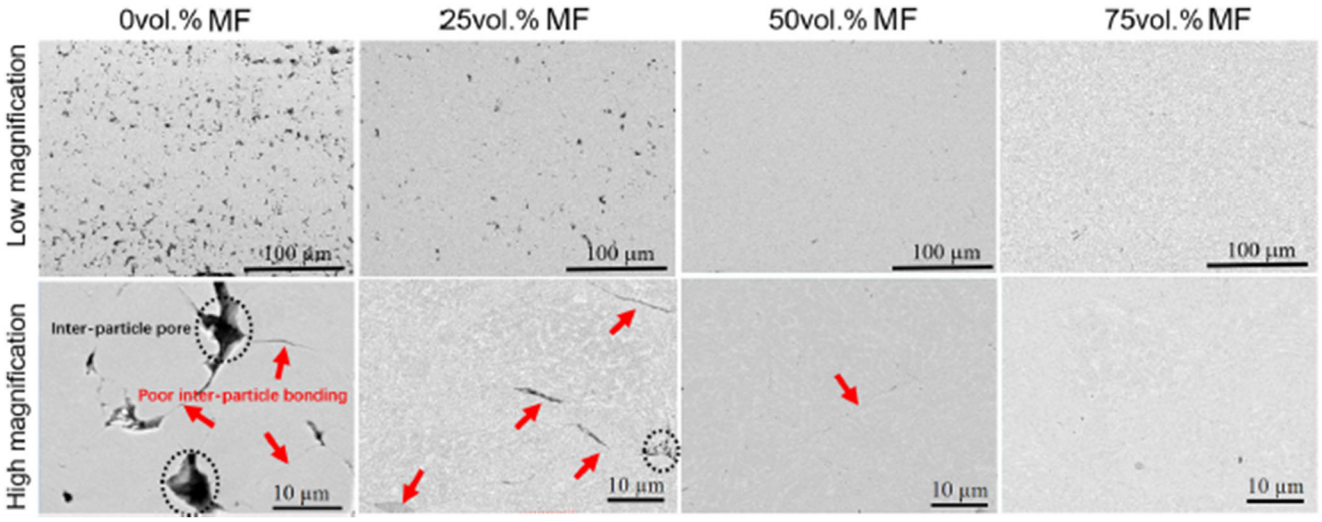

Fig. 15 SPD coating of Inconel 718 containing stainless-steel particles. As the %vol of stainless-steel particles increased, the porosity of coating was reduced, showing higher inter-particle bonding [25]

assisting flux on Al tubes and fins, and finally brazing process. However, the SPD process could eliminate these complex mid-processes. Thick and relatively dense layers of Zn and flux (without phase transformation, oxidation, and microstructure change) can be easily produced using the SPD process [69, 72].

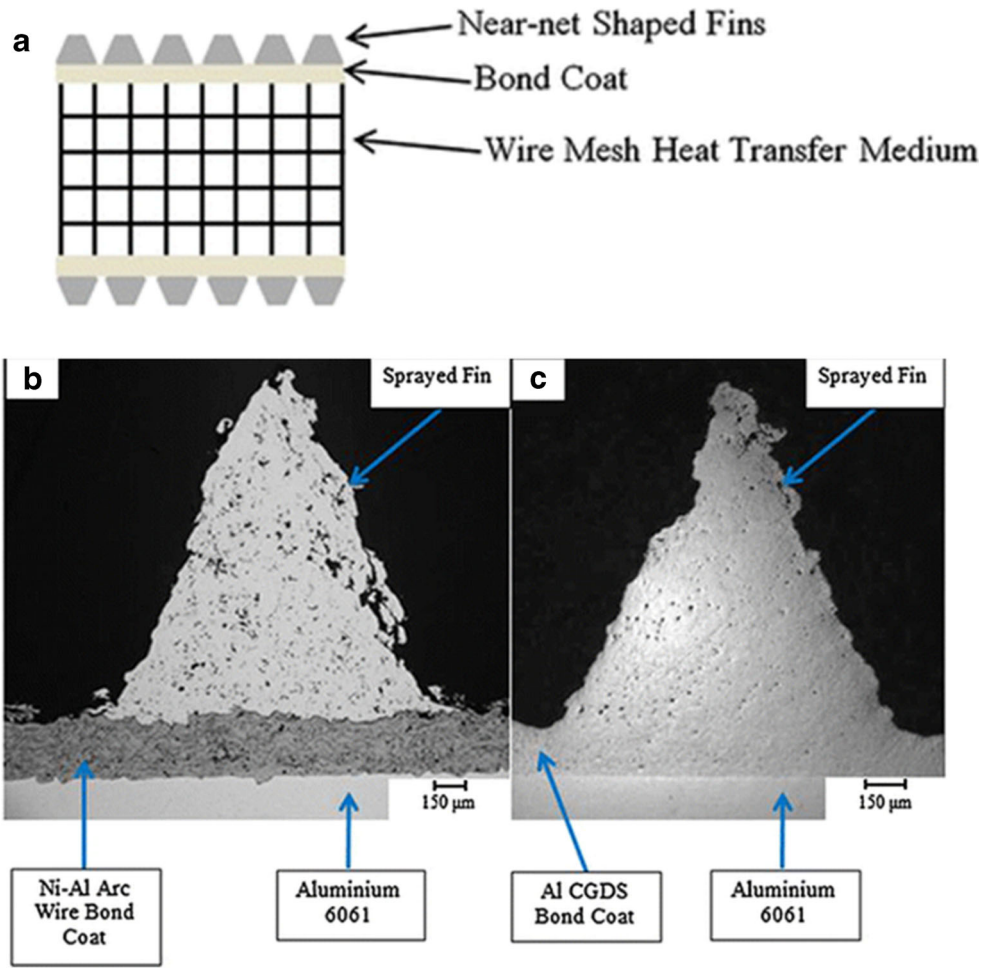

Fig. 16 A simple example of a 3D bulk-scale deposit employing SPD additive manufacturing. **a** Schematic illustration of the improved wire heat exchanger; SPD 3D fins on different metallic bond coatings. **b** Ni–Al bond coating. **c** Al bond coating [65, 69]

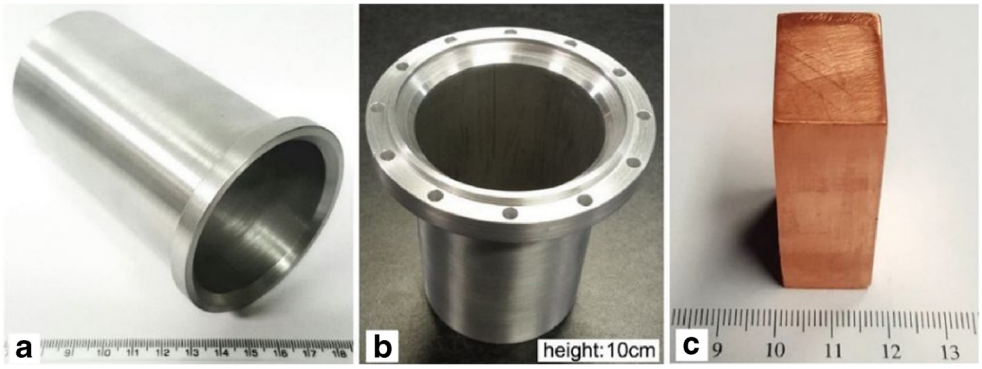

Fig. 17 Finished part fabricated by machining of SPD produced parts. **a** Aluminum alloy tube. **b** Aluminum alloy flange. **c** Copper cuboid [71]

Recently, electrically conductive thick metallic tracks can be easily and quickly formed on the plastic mold parts (with complex shapes) using the SPD process. These metallic tracks deposited on plastic components also exhibited high denseness and electrical conductivity as well. In fact, coatings deposited by arc, combustion (flame), plasma, and high-velocity oxygen fuel (HVOF) spraying processes displayed 50–200% lower electrical conductivity than SPD deposits. This problem is mainly related to the presence of defects such as pores and oxides in the deposit microstructure (produced by thermal and plasma spray processes). In this regard, Bonzin et al. [69, 73] deposited a Cu layer by SPD on an open mold. Injection molding was then accomplished when the mold was closed. The Cu layer was then transferred to the molded plastic component to produce a hybrid Cu/plastic part.

Dimensional repair and refurbishment in the aerospace and defense sectors have recently started utilizing SPD technology as a cost-effective process (particularly when N_2 is used as propellant gas). In fact, oxide-free deposits with hundreds of micrometer thickness and strong adhesion to the substrate (per tensile adhesion tests) and often higher hardness than original powder can be produced using the SPD process [74]. Also, commercially pure Al was sprayed on the Mg alloy to lessen the corrosion pits on the helicopter tail [69]. Figure 19 demonstrates the 3D repair of the transmission tee box which is made by cast Al. It is clearly seen that the damaged area of this component can be easily refurbished using the SPD process [69].

4.1.3 Disadvantages of SPD as an additive manufacturing

Tariq et al. [30] showed that there are some disadvantages to SPD as an additive manufacturing process. To use harder materials, pressures need to be increased, and nitrogen or helium needs to be used as propellants. The necessary inclusion of expensive pressurized propellants is one of the reasons that SPD has been slow to appear in industry. However, Raoelison et al. [75] explained that SPD, when used as an additive manufacturing process, can lead to reduced manufacturing costs, and reduced material consumption.

4.1.4 Innovations and improvements

Because the SPD is a young process, there are still many aspects that can be innovated and improved upon. Faizan-Ur-Rab [37] explained that to obtain greater efficiency in the SPD as an additive manufacturing process, a 3D model is needed to calculate the particle acceleration and impact temperature. The 3D model can also predict particle flow as a function of particle size, temperature, and velocity and can account for the path of individual particles within the nozzle. The 3D model can be used to save costs and develop more accurate SPD additive manufacturing processes [37].

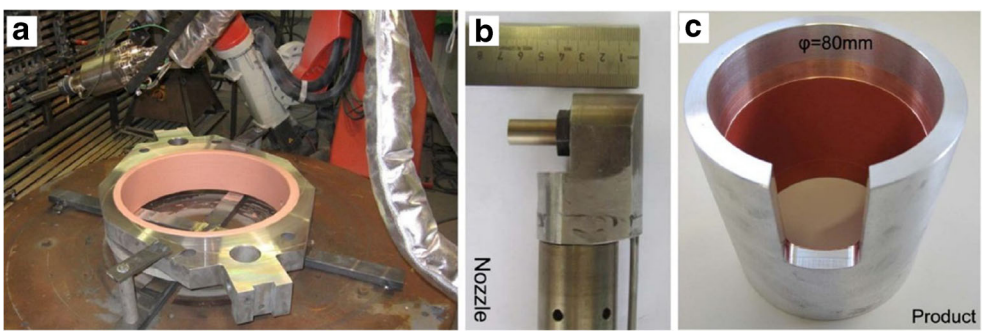

Fig. 18 SPD/CSAM rotational structure. **a** An inner wall of a pressure ring for food processing machine. **b** A small-size cold spray nozzle. **c** An inner wall of small-space cylinder tube [71]

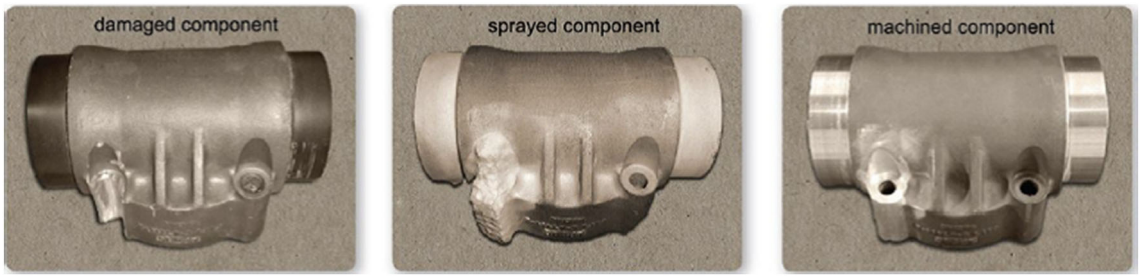

Fig. 19 3D repair of transmission tee box (which is made by cast Al) [69, 71]

4.2 Applications in various other fields

4.2.1 Energetic material coatings

SPD can be used to create coatings made of energetic materials. Energetic materials have high amounts of stored chemical energy that can be released through ignition, such as laser ignition, and these sorts of materials are used in explosives, rocket fuels, and pyrotechnics. Using SPD, Dean et al. [13] manufactured fully dense energetic material coatings that had microstructures similar to the spray powder. This research showed that using the SPD to create energetic coatings can result in parts made completely of energetic materials. Attempts have been made to create these energetic SPD coatings using nitrogen instead of the more expensive helium, through the use of nickel-clad aluminum powders as binders in the coating. Altering the coating composition and density allows the propagation rate to be varied, which enables fine-tuning to the ignition properties.

4.2.2 Electrical components

The SPD has applications for electrical components. Tazegul et al. [76] explained that when using copper and Al_2Cu powders, the ideal range of copper for wear reduction and electrical conductivity is to have between 5 and 10%. When coatings exceed 15 vol.% of copper, there is a decrease in conductivity and wear resistance. SPD can be used to create a composite coating that performs similar to bulk copper. The composites have higher wear resistance but are still electrically conductive. These composite coatings often perform better than a simple copper coating, both electrically and tribologically [76]. Li et al. [45] stated that when a sprayed coating is fully dense, there is improved thermal conductivity, improved electrical conductivity, and higher anti-corrosion properties.

Carbon nanotubes can be used to improve heat conductivity and thermal conductivity. Bakshi et al. [60] explained that carbon nanotubes are used as reinforcement for the SPD coatings. However, the tubes can fracture during deposition. Cho et al. [26] explained that because carbon nanotubes can be damaged by the high heat of other coating methods, the SPD technique is an excellent choice to deposit carbon nanotube in metal matrix composites coatings.

Gärtner et al. [43] explained that because SPD coatings have few defects, the coatings produced resembles the electrical or thermal conductivity of the bulk material used.

4.2.3 Aerospace applications

SPD technique is of great interest to the aerospace industry due to its higher coating density [64]. Because it can overcome oxidation drawbacks [77] and is low cost, it is attractive in the potential repair of components and shows promise in maintenance applications [17]. Ajaja et al. [36] have found that SPD coatings can help disperse heat in engines and that titanium is effective for this use. Titanium is light-weight and corrosion-resistant, which makes it an excellent potential coating material for rocket engines. Titanium SPD coatings were shown to have higher true hardness than other coatings. Dense titanium SPD coatings were shown to have similar properties to bulk titanium. SPD technique has the potential for creating titanium parts if the number of micro defects can be reduced or eliminated [36].

4.2.4 Low-pressure SPD for component repair

Low-pressure SPD can be used to repair damaged and worn components. Because high-pressure systems are too expensive to be deployed in industry, much research is being done on using low-pressure systems and more diverse materials to bring the cost of manufacturing down. Petrackova et al. [31] showed that SPD could be used to extend the expected lifespan of parts that are already in use, which has applications in air travel. The SPD process uses less power than other methods like welding or plasma spraying and is particularly useful for dimensional restoration. Dimensional restoration repair requirements are not as stringent as the requirements for load-bearing components. Cavities on machine parts or components can be filled using SPD. These filled cavities produce fatigue test results that are similar to the bulk material. Low-pressure SPD can be used to fill cavities of varying shapes. This SPD filling alleviates the stress accumulation of certain shapes [31].

As SPD limits oxidation, it allows for higher-purity composite coatings to be formed. The SPD has been used to repair metal sculptures as well as create complex geometry, decorative accents, and even original works of art [75].

4.2.5 Reduce corrosion and wear

Corrosion and wear are two of the biggest problems affecting component lifespan, and many SPD materials can be used to protect against these two problems. Brewer et al. [11] explained that pure aluminum and stainless steel SPD coatings had been used to achieve corrosion resistance on magnesium and aluminum. Deposition efficiency has been increased to nearly 100% by using mixed particle sizes, adding additional particles of aluminum oxide powder and increasing the temperature to increase the velocity and pressure [11]. Cong et al. [27] studied that materials that are subject to high levels of corrosion, such as those in marine environments, can benefit from SPD. When steel was coated by SPD with aluminum and Al_2O_3 particles, it protected the steel from corrosion. Even after 960 h of neutral salt spray corrosion simulation, the SPD coating was still effective as a barrier against corrosion for the substrate.

Huang et al. [78] used Muntz brass alloy (Cu60Zn40) for its corrosion resistance. When compared to vacuum plasma spraying, SPD showed coating materials that are closer to the original powder than vacuum plasma spraying materials. Microhardness is higher with SPD compared to vacuum plasma spraying. The substrates after SPD typically displayed bigger grain size and flatter grains compared to the substrates that were vacuum plasma sprayed [78]. Qiu et al. [34] explained that hard ceramic or metal particles had been added to the SPD feedstock to improve the coating quality. In regard to added materials, typically, finer particles provide lower wear rates than coarser particles. The smaller particles result in higher hardness of the coating which reduces the friction coefficient. Aluminum oxide (Al_2O_3) is a material commonly added to SPD feedstock. Aluminum oxide (Al_2O_3) is a popular coating for automotive and aerospace applications. As the amount of Al_2O_3 in the feedstock was increased, the coating became less and less rough. Figure 20 shows the surface topography of five coatings with varying amounts of Al_2O_3 sprayed on an AZ31 magnesium alloy substrate.

Alidokht et al. [29] explained that tungsten carbide (WC) coatings are resistant to wear. These coatings are typically applied through laser cladding. Laser cladding can cause a non-homogenous distribution of WC particles and considerable residual stress, resulting in reduced wear resistance. SPD is an ideal method for creating these coatings. In their study, WC and Ni were fed into the nozzle using different feed rates in separate hoppers. The WC particles decreased the porosity of the coating; however, the WC particles also decreased the deposition efficiency. The WC particles decreased the coefficient of friction and wear rate by a factor of seven. These improvements were a result of the stable and cohesive mechanically mixed

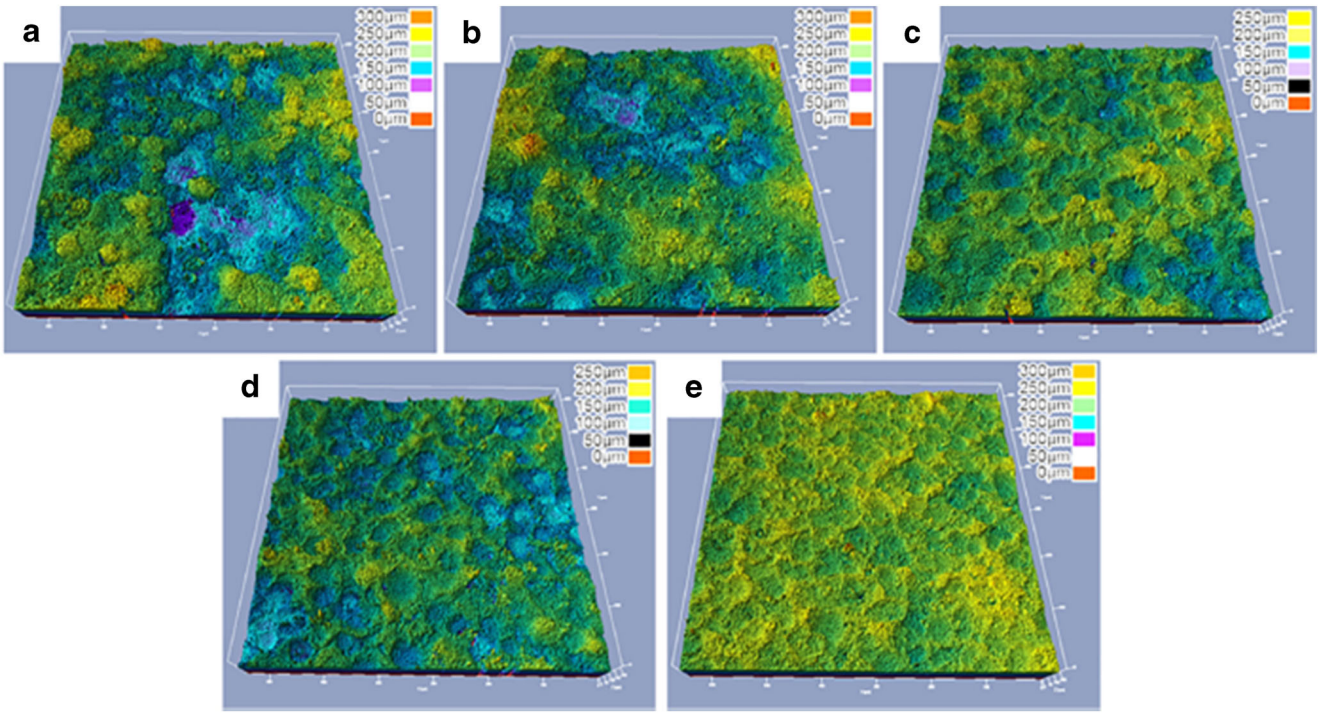

Fig. 20 Surface topography of five coatings with varying amounts of Al_2O_3. **a** Zero percent Al_2O_3 or pure A380 aluminum alloy powder. **b** Ten percent Al_2O_3. **c** Twenty percent Al_2O_3. **d** Thirty percent Al_2O_3, (e) 40% Al_2O_3 [34]

layer on the wear track comprised of WC-Ni. This mechanically mixed layer protected the sample from wear. As the small particles of WC broke off during the scratch test, they were further incorporated into the mechanically mixed layer [29].

Yin et al. [79] discussed that WC-Co-Ni coatings could be challenging to work with because they typically require more expensive accelerants and increased operating temperatures. However, by using porous WC-Co powders and a mix of dense Ni powders to act as binders, the authors were able to create very high deposition efficiency and high WC retention, due to the fracture of the porous WC-Co particles. The hardness and wear resistance increased with the addition of WC content. Because these porous WC-Co particles do not require the expensive accelerants, this method could be employed as a lower-cost method to create WC coatings [79].

Watson et al. [80] explained that SPD technique could be used to make quasi-crystal reinforced nanocomposite coatings. The nanocomposites are made up of Al–Cr–Mn–Co–Zr on an aluminum substrate. These coatings show excellent resistance to corrosion, including salt fog-induced pitting corrosion. The coatings also show no evidence of galvanic couples with adjacent exposed areas.

4.2.6 Self-lubricating metal matrix composites

SPD can be used to create self-lubricating coatings. Zhang et al. [28] suggested that other coating methods can cause damage to the solid lubricants when manufacturing self-lubricating metal matrix composites. Zhang et al. [28] found that SPD is a preferred method for manufacturing self-lubricating metal matrix composites because it does not damage the solid lubricants. The authors prepared two coatings Cu-MoS_2 and Cu-MoS_2-WC on aluminum alloy AA6061. The coatings were sprayed using nitrogen as a carrier gas at a pressure of 5 MPa at 800 °C. Cu-MoS_2 coatings by SPD performed similarly to other Cu-MoS_2 coatings. However, Cu-MoS_2-WC coatings had smaller detachments. Further WC particles continued to be found incorporated into the wear track even after 1000 cycles. These WC particles reduce friction because the WC particles are the load-bearing particles. The WC particles helped to form a stable tribolayer [28]. Figure 21 shows the wear track of Cu-MoS_2 coating and a wear track of Cu-MoS_2-WC coating. Both coatings show wear track after 100 cycles and 1000 cycles.

4.2.7 Neutron shielding

The SPD technique has applications in neutron shielding. B4C/Al composites are good neutron shielding materials that can be used for nuclear applications, such as storing spent nuclear fuel. While other materials used for neutron shielding are hazardous to work with, B4C/Al is not, and is especially effective for wet nuclear storage applications. Tariq et al. [30] deposited a 6-mm thick neutron shielding coating made of B4C/Al composite sprayed onto the 6061-T6 Al substrate. The coatings were brittle after heat treatment at 200 °C. However, when heat treatment temperature was increased to 500 °C, the coatings demonstrated maximum ductility. This heat treatment was also shown to have minimal effect on the neutron shielding capability. The neutron shielding showed increased attenuation as the thickness of the coating increased. A sample with a coating thickness of 5 mm was heat-treated to 500 °C and showed between 50 and 55% attenuation.

5 Conclusions

Since its discovery in the 1980s, the SPD has developed into a refined method for coating substrates through the application of multiple layers of sprayed particles. These coatings can provide protection from wear and corrosion, increase electrical conductivity, and even repair damaged components. SPD is a solid-state process as it is performed below the melting point temperatures and has many advantages over other coating methods.

The properties of SPD materials and processing parameters impact the outcome. The ratio DE defines efficiency. Higher DE

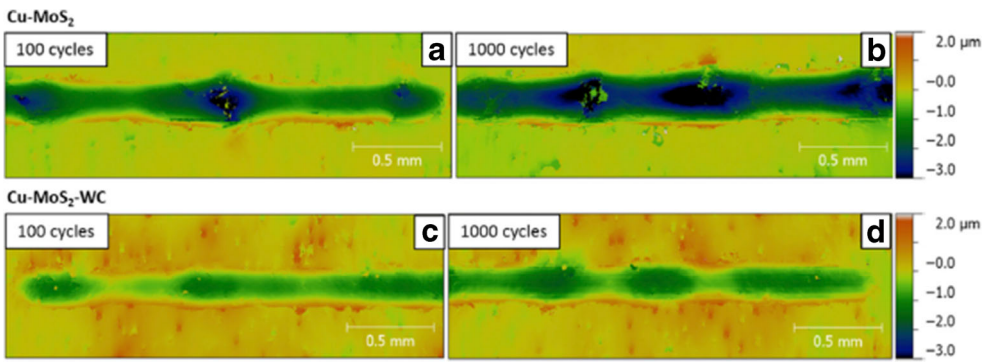

Fig. 21 The wear tray for Cu-MoS_2 (**a**, **b**), and Cu-MoS_2WC (**c**, **d**) [28]

is preferred as it is more efficient and cost-effective. SPD methods are classified by two types: high and low pressure, and coatings can be made from a combination of metals, ceramics, and polymers.

Velocity also affects the impact and deformity of sprayed particles. Higher velocity typically results in higher DE. Helium is the preferred carrier gas, but as it is the most expensive, nitrogen and compressed air are more commonly used as affordable carriers. Critical velocity is the minimum velocity necessary for the SPD particles to adhere; however, once erosion velocity is surpassed, the particles will erode at the substrate. In addition to the velocity, the spray angle can affect coating quality. Pre-processing the spray particles can enhance the microstructure of the finished coating. Cold worked particles have a finer microstructure than non-cold worked particles. SPD coating performance depends on the type of substrate used, as well as the particle properties. A wide variety of materials are used in SPD, and this paper has mentioned some of the most common materials used. In SPD technique, there are two bonding mechanisms: metal-to-metal bonding and mechanical interlocking; each is important to the strength of the finished coating.

SPD technique faces challenges such as voids. However, these can be tamped down by larger peening particles. Particle shape is important as spherical spray particles adhere better than particles with a dendrite-like shape. Some extra consideration needs to be given when creating SPD coatings that use carbon nanotubes, as these tubes may break upon impact during the spray process.

The potential applications of SPD are vast. Specific applications include energetic material coatings, electrical components, component repair, tribological coatings, self-lubricating composite coatings, additive manufacturing, and more. SPD is still considered a young technology; however, the SPD has many potential applications. These include electronics, marine, tribological coatings, biomedical, aerospace, and nuclear industries.

References

1. Zhou HX, Li CX, Ji G, Fu SL, Yang H, Luo XT, Yang GJ, Li CJ (2018) Local microstructure inhomogeneity and gas temperature effect in in-situ shot-peening assisted cold-sprayed Ti-6Al-4V coating. J Alloys Compd 766:694–704. https://doi.org/10.1016/j.jallcom.2018.07.009
2. Stoltenhoff T, Kreye H, Richter HJ (2002) An analysis of the cold spray process and its coatings. J Therm Spray Technol 11(4):542–550. https://doi.org/10.1361/105996302770348682
3. Assadi H, Kreye H, Gartner F, Klassen T (2016) Cold spraying - a materials perspective. Acta Mater 116:382–407. https://doi.org/10.1016/j.actamat.2016.06.034
4. Sova A, Maestracci R, Jeandin M, Bertrand P, Smurov I (2017) Kinetics of composite coating formation process in cold spray: modelling and experimental validation. Surf Coat Technol 318:309–314. https://doi.org/10.1016/j.surfcoat.2016.06.084
5. Borchers C, Gartner F, Stoltenhoff T, Assadi H, Kreye H (2003) Microstructural and macroscopic properties of cold sprayed copper coatings. J Appl Phys 93(12):10064–10070. https://doi.org/10.1063/1.1573740
6. Dosta S, Bolelli G, Candeli A, Lusvarghi L, Cano IG, Guilemany JM (2017) Plastic deformation phenomena during cold spray impact of WC-Co particles onto metal substrates. Acta Mater 124:173–181. https://doi.org/10.1016/j.actamat.2016.11.010
7. Vilardell AM, Cinca N, Dosta S, Cano IG, Guilemany JM (2019) Feasibility of using low pressure cold gas spray for the spraying of thick ceramic hydroxyapatite coatings. Int J Appl Ceram Technol 16(1):221–229. https://doi.org/10.1111/ijac.13088
8. Meng FC, Hu DY, Gao Y, Yue S, Song J (2016) Cold-spray bonding mechanisms and deposition efficiency prediction for particle/substrate with distinct deformability. Mater Des 109:503–510. https://doi.org/10.1016/j.matdes.2016.07.103
9. Moridi A, Hassani-Gangaraj SM, Guagliano M, Dao M (2014) Cold spray coating: review of material systems and future perspectives. Surf Eng 30(6):369–U329. https://doi.org/10.1179/1743294414y.0000000270
10. Villa M, Dosta S, Guilemany JM (2013) Optimization of 316L stainless steel coatings on light alloys using cold gas spray. Surf Coat Technol 235:220–225. https://doi.org/10.1016/j.surfcoat.2013.07.036
11. Brewer LN, Schiel JF, Menon ESK, Woo DJ (2018) The connections between powder variability and coating microstructures for cold spray deposition of austenitic stainless steel. Surf Coat Technol 334:50–60. https://doi.org/10.1016/j.surfcoat.2017.10.082
12. Spencer K, Luzin V, Matthews N, Zhang MX (2012) Residual stresses in cold spray Al coatings: the effect of alloying and of process parameters. Surf Coat Technol 206(19-20):4249–4255. https://doi.org/10.1016/j.surfcoat.2012.04.034
13. Dean SW, Potter JK, Yetter RA, Eden TJ, Champagne V, Trexler M (2013) Energetic intermetallic materials formed by cold spray. Intermetallics 43:121–130. https://doi.org/10.1016/j.intermet.2013.07.019
14. Schmidt T, Gartner F, Assadi H, Kreye H (2006) Development of a generalized parameter window for cold spray deposition. Acta Mater 54(3):729–742. https://doi.org/10.1016/j.actamat.2005.10.005
15. Moridi A, Hassani-Gangaraj SM, Guagliano M (2013) A hybrid approach to determine critical and erosion velocities in the cold spray process. Appl Surf Sci 273:617–624. https://doi.org/10.1016/j.apsusc.2013.02.089
16. Schmidt T, Assadi H, Gartner F, Richter H, Stoltenhoff T, Kreye H, Klassen T (2009) From particle acceleration to impact and bonding in cold spraying. J Therm Spray Technol 18(5-6):794–808. https://doi.org/10.1007/s11666-009-9357-7
17. Jenkins R, Yin S, Aldwell B, Meyer M, Lupoi R (2018) New insights into the in-process densification mechanism of cold spray Al coatings: low deposition efficiency induced densification. J Mater Sci Technol
18. Xiong YM, Bae G, Xiong X, Lee C (2010) The effects of successive impacts and cold welds on the deposition onset of cold spray coatings. J Therm Spray Technol 19(3):575–585. https://doi.org/10.1007/s11666-009-9455-6
19. Wang XM, Feng F, Klecka MA, Mordasky MD, Garofano JK, El-Wardany T, Nardi A, Champagne VK (2015) Characterization and modeling of the bonding process in cold spray additive manufacturing. Additive Manufacturing 8:149–162. https://doi.org/10.1016/j.addma.2015.03.006
20. Ajdelsztajn L, Jodoin B, Kim GE, Schoenung JM (2005) Cold spray deposition of nanocrystalline aluminum alloys. Metallurgical and Materials Transactions a-Physical Metallurgy

and Materials Science 36A(3):657–666. https://doi.org/10.1007/s11661-005-0182-4
21. Liu JC, Cui H, Zhou XL, Wu XK, Zhang JS (2012) Nanocrystalline copper coatings produced by cold spraying. Met Mater Int 18(1): 121–128. https://doi.org/10.1007/s12540-012-0014-1
22. Ito K, Ichikawa Y (2019) Microstructure control of cold-sprayed pure iron coatings formed using mechanically milled powder. Surf Coat Technol 357:129–139. https://doi.org/10.1016/j.surfcoat.2018.10.016
23. Ajdelsztajn L, Jodoin B, Schoenung JM (2006) Synthesis and mechanical properties of nanocrystalline Ni coatings produced by cold gas dynamic spraying. Surf Coat Technol 201(3-4):1166–1172. https://doi.org/10.1016/j.surfcoat.2006.01.037
24. Rokni MR, Widener CA, Crawford GA, West MK (2015) An investigation into microstructure and mechanical properties of cold sprayed 7075 Al deposition. Materials Science and Engineering a-Structural Materials Properties Microstructure and Processing 625: 19–27. https://doi.org/10.1016/j.msea.2014.11.059
25. Luo XT, Yao ML, Ma N, Takahashi M, Li CJ (2018) Deposition behavior, microstructure and mechanical properties of an in-situ micro-forging assisted cold spray enabled additively manufactured Inconel 718 alloy. Mater Des 155:384–395. https://doi.org/10.1016/j.matdes.2018.06.024
26. Cho SC, Takagi K, Kwon H, Seo D, Ogawa K, Kikuchi K, Kawasaki A (2012) Multi-walled carbon nanotube-reinforced copper nanocomposite coating fabricated by low-pressure cold spray process. Surf Coat Technol 206(16):3488–3494. https://doi.org/10.1016/j.surfcoat.2012.02.021
27. Cong DL, Li ZS, He QB, Chen HB, Zhao ZP, Zhang LP, Wu HL (2017) Wear behavior of corroded Al-Al2O3 composite coatings prepared by cold spray. Surf Coat Technol 326:247–254. https://doi.org/10.1016/j.surfcoat.2017.07.063
28. Zhang YY, Epshteyn Y, Chromik RR (2018) Dry sliding wear behaviour of cold-sprayed Cu-MoS2 and Cu-MoS2-WC composite coatings: the influence of WC. Tribol Int 123:296–306. https://doi.org/10.1016/j.triboint.2017.12.015
29. Alidokht SA, Manimunda P, Vo P, Yue S, Chromik RR (2016) Cold spray deposition of a Ni-WC composite coating and its dry sliding wear behavior. Surf Coat Technol 308:424–434. https://doi.org/10.1016/j.surfcoat.2016.09.089
30. Tariq NH, Gyansah L, Wang JQ, Qiu X, Feng B, Siddique MT, Xiong TY (2018) Cold spray additive manufacturing: a viable strategy to fabricate thick B4C/Al composite coatings for neutron shielding applications. Surf Coat Technol 339:224–236. https://doi.org/10.1016/j.surfcoat.2018.02.007
31. Petrackova K, Kondas J, Guagliano M (2018) Fixing a hole (with cold spray). Int J Fatigue 110:144–152. https://doi.org/10.1016/j.ijfatigue.2018.01.014
32. Kumar S, Bae G, Lee C (2016) Influence of substrate roughness on bonding mechanism in cold spray. Surf Coat Technol 304:592–605. https://doi.org/10.1016/j.surfcoat.2016.07.082
33. Yin S, Yan XC, Chen CY, Jenkins R, Liu M, Lupoi R (2018) Hybrid additive manufacturing of Al-Ti6Al4V functionally graded materials with selective laser melting and cold spraying. J Mater Process Technol 255:650–655. https://doi.org/10.1016/j.jmatprotec.2018.01.015
34. Qiu X, Tariq NU, Wang JQ, Tang JR, Gyansah L, Zhao ZP, Xiong TY (2018) Microstructure, microhardness and tribological behavior of Al2O3 reinforced A380 aluminum alloy composite coatings prepared by cold spray technique. Surf Coat Technol 350:391–400. https://doi.org/10.1016/j.surfcoat.2018.07.039
35. Lek JY, Bhowmik A, Tan AWY, Sun W, Song X, Zhai W, Buenconsejo PJ, Li F, Liu EJ, Lam YM, Boothroyd CB (2018) Understanding the microstructural evolution of cold sprayed Ti-6Al-4V coatings on Ti-6Al-4V substrates. Appl Surf Sci 459: 492–504. https://doi.org/10.1016/j.apsusc.2018.07.175
36. Ajaja J, Goldbaum D, Chromik RR (2011) Characterization of Ti cold spray coatings by indentation methods. Acta Astronautica 69(11-12):923–928. https://doi.org/10.1016/j.actaastro.2011.06.012
37. Faizan-Ur-Rab M, Zahiri SH, Masood SH, Phan TD, Jahedi M, Nagarajah R (2016) Application of a holistic 3D model to estimate state of cold spray titanium particles. Mater Des 89:1227–1241. https://doi.org/10.1016/j.matdes.2015.10.075
38. Arabgol Z, Vidaller MV, Assadi H, Gartner F, Klassen T (2017) Influence of thermal properties and temperature of substrate on the quality of cold-sprayed deposits. Acta Mater 127:287–301. https://doi.org/10.1016/j.actamat.2017.01.040
39. King PC, Busch C, Kittel-Sherri T, Jahedi M, Gulizia S (2014) Interface melding in cold spray titanium particle impact. Surf Coat Technol 239:191–199. https://doi.org/10.1016/j.surfcoat.2013.11.039
40. Hussain T, McCartney DG, Shipway PH, Zhang D (2009) Bonding mechanisms in cold spraying: the contributions of metallurgical and mechanical components. J Therm Spray Technol 18(3):364–379. https://doi.org/10.1007/s11666-009-9298-1
41. Xie YC, Yin S, Chen CY, Planche MP, Liao HL, Lupoi R (2016) New insights into the coating/substrate interfacial bonding mechanism in cold spray. Scr Mater 125:1–4. https://doi.org/10.1016/j.scriptamat.2016.07.024
42. Nikbakht R, Seyedein SH, Kheirandish S, Assadi H, Jodoin B (2018) Asymmetrical bonding in cold spraying of dissimilar materials. Appl Surf Sci 444:621–632. https://doi.org/10.1016/j.apsusc.2018.03.103
43. Gartner F, Stoltenhoff T, Schmidt T, Kreye H (2006) The cold spray process and its potential for industrial applications. J Therm Spray Technol 15(2):223–232. https://doi.org/10.1361/105996306x108110
44. Leitz KH, O'Sullivan M, Plankensteiner A, Kestler H, Sigl LS (2018) OpenFOAM modeling of particle heating and acceleration in cold spraying. J Therm Spray Technol 27(1-2):135–144. https://doi.org/10.1007/s11666-017-0644-4
45. Li YJ, Luo XT, Rashid H, Li CJ (2018) A new approach to prepare fully dense Cu with high conductivities and anti-corrosion performance by cold spray. J Alloys Compd 740:406–413. https://doi.org/10.1016/j.jallcom.2017.11.053
46. Winnicki M, Malachowska A, Piwowarczyk T, Rutkowska-Gorczyca M, Ambroziak A (2016) The bond strength of Al + Al2O3 cermet coatings deposited by low-pressure cold spraying. Arch Civil Mech Eng 16(4):743–752. https://doi.org/10.1016/j.acme.2016.04.014
47. Malachowska A, Winnicki M, Konat L, Piwowarczyk T, Pawlowski L, Ambroziak A, Stachowicz M (2017) Possibility of spraying of copper coatings on polyamide 6 with low pressure cold spray method. Surf Coat Technol 318:82–89. https://doi.org/10.1016/j.surfcoat.2017.02.001
48. Feng Y, Li WY, Guo CW, Gong MJ, Yang K (2018) Mechanical property improvement induced by nanoscaled deformation twins in cold-sprayed Cu coatings. Materials Science and Engineering a-Structural Materials Properties Microstructure and Processing 727:119–122. https://doi.org/10.1016/j.msea.2018.04.113
49. Lee YTR, Ashrafizadeh H, Fisher G, McDonald A (2017) Effect of type of reinforcing particles on the deposition efficiency and wear resistance of low-pressure cold-sprayed metal matrix composite coatings. Surf Coat Technol 324:190–200. https://doi.org/10.1016/j.surfcoat.2017.05.057
50. Huang CJ, Li WY, Xie YC, Planche MP, Liao HL, Montavon G (2017) Effect of substrate type on deposition behavior and wear performance of ni-coated graphite/al composite coatings deposited by cold spraying. J Mater Sci Technol 33(4):338–346. https://doi.org/10.1016/j.jmst.2016.11.016

51. Kumar S, Reddy SK, Joshi SV (2017) Microstructure and performance of cold sprayed Al-SiC composite coatings with high fraction of particulates. Surf Coat Technol 318:62–71. https://doi.org/10.1016/j.surfcoat.2016.11.047
52. Na H, Bae G, Shin S, Kumar S, Kim H, Lee C (2009) Advanced deposition characteristics of kinetic sprayed bronze/diamond composite by tailoring feedstock properties. Compos Sci Technol 69(3-4):463–468. https://doi.org/10.1016/j.compscitech.2008.11.015
53. Kwon H, Cho S, Kawasaki A (2015) Diamond-reinforced metal matrix bulk materials fabricated by a low-pressure cold-spray process. Mater Trans 56 (1):108-112. doi:https://doi.org/10.2320/matertrans.M2014145
54. Tang J, Saha GC, Richter P, Kondas J, Colella A, Matteazzi P (2018) Effects of post-spray heat treatment on hardness and wear properties of Ti-WC high-pressure cold spray coatings. J Therm Spray Technol 27(7):1153–1164. https://doi.org/10.1007/s11666-018-0762-7
55. Peat T, Galloway A, Toumpis A, McNutt P, Iqbal N (2017) The erosion performance of particle reinforced metal matrix composite coatings produced by co-deposition cold gas dynamic spraying. Appl Surf Sci 396:1623–1634. https://doi.org/10.1016/j.apsusc.2016.10.155
56. Ji GC, Wang HT, Chen X, Bai XB, Dong ZX, Yang FG (2013) Characterization of cold-sprayed multimodal WC-12Co coating. Surf Coat Technol 235:536–543. https://doi.org/10.1016/j.surfcoat.2013.08.021
57. Yandouzi M, Bu H, Brochu M, Jodoin B (2012) Nanostructured Al-based metal matrix composite coating production by pulsed gas dynamic spraying process. J Therm Spray Technol 21(3-4):609–619. https://doi.org/10.1007/s11666-011-9727-9
58. Al-Hamdani KS, Murray JW, Hussain T, Kennedy A, Clare AT (2017) Cold sprayed metal-ceramic coatings using satellited powders. Mater Lett 198:184–187. https://doi.org/10.1016/j.matlet.2017.03.175
59. Sova A, Kosarev V, Papyrin A, Smurov I (2011) Effect of ceramic particle velocity on cold spray deposition of metal-ceramic coatings. J Therm Spray Technol 20(1-2):285–291. https://doi.org/10.1007/s11666-010-9571-3
60. Bakshi SR, Singh V, Balani K, McCartney DG, Seal S, Agarwal A (2008) Carbon nanotube reinforced aluminum composite coating via cold spraying. Surf Coat Technol 202(21):5162–5169. https://doi.org/10.1016/j.surfcoat.2008.05.042
61. Bagherifard S, Monti S, Zuccoli MV, Riccio M, Kondas J, Guagliano M (2018) Cold spray deposition for additive manufacturing of freeform structural components compared to selective laser melting. Materials Science and Engineering a-Structural Materials Properties Microstructure and Processing 721:339–350. https://doi.org/10.1016/j.msea.2018.02.094
62. Yang K, Li WY, Guo XP, Yang XW, Xu YX (2018) Characterizations and anisotropy of cold-spraying additive-manufactured copper bulk. J Mater Sci Technol 34(9):1570–1579. https://doi.org/10.1016/j.jmst.2018.01.002
63. Jing Z, Dejun K (2018) Effect of laser remelting on microstructure and immersion corrosion of cold-sprayed aluminum coating on S355 structural steel. Opt Laser Technol 106:348–356. https://doi.org/10.1016/j.optlastec.2018.04.026
64. Daroonparvar R, Kay CM, Karthikeyan J (2018) Modified bond coatings improve service life of plasma sprayed thermal barrier coatings and protective performance of overlay coatings. Adv Mater Process 176(5):40–43
65. Cormier Y, Dupuis P, Jodoin B, Corbeil A (2015) Mechanical properties of cold gas dynamic-sprayed near-net-shaped fin arrays. J Therm Spray Technol 24(3):476–488. https://doi.org/10.1007/s11666-014-0203-1
66. Pattison J, Celotto S, Morgan R, Bray M, O'Neill W (2007) Cold gas dynamic manufacturing: a non-thermal approach to freeform fabrication. Int J Mach Tool Manu 47(3-4):627–634. https://doi.org/10.1016/j.ijmachtools.2006.05.001
67. Lynch M, Gu W, El-Wardany T, Hsu A, Viens D, Nardi A, Klecka M (2013) Design and topology/shape structural optimization for additively manufactured cold sprayed components. Virtual Phys Prototy 8:213–231. https://doi.org/10.1080/17452759.2013.837629
68. Sova A, Grigoriev S, Okunkova A, Smurov I (2013) Potential of cold gas dynamic spray as additive manufacturing technology. Int J Adv Manuf Technol 69(9-12):2269–2278. https://doi.org/10.1007/s00170-013-5166-8
69. High Pressure Cold Spray: Principles and Applications (2016). ASM International,
70. Li WY, Li CJ, Liao HL (2006) Effect of annealing treatment on the microstructure and properties of cold-sprayed Cu coating. J Therm Spray Technol 15(2):206–211. https://doi.org/10.1361/105996306x108066
71. Yin S, Cavaliere P, Aldwell B, Jenkins R, Liao HL, Li WY, Lupoi R (2018) Cold spray additive manufacturing and repair: fundamentals and applications. Additive Manufacturing 21:628–650. https://doi.org/10.1016/j.addma.2018.04.017
72. Yoon SH, Lee C, Kim HJ Process development of brazed aluminum heat exchanger using a kinetic spraying process. In: International Thermal Spray Conference, Beijing, China, 2007. Global Coating Solutions. ASM International, p 1180
73. Bobzin K, Öte M, Linke TF, Aachen R Integration of electrical functionality by transplantation of cold sprayed electrical conductive Cu tracks via injection moulding. In: International Thermal Spray Conference, Barcelona, Spain, 2014. ASM International, p 6
74. Murray JW, Zuccoli MV, Hussain T (2018) Heat treatment of cold-sprayed C355 Al for repair: microstructure and mechanical properties. J Therm Spray Technol 27(1-2):159–168. https://doi.org/10.1007/s11666-017-0665-z
75. Raoelison RN, Verdy C, Liao H (2017) Cold gas dynamic spray additive manufacturing today:deposit possibilities, technological solutions and viable applications. Mater Des 133:266-287. doi: https://doi.org/10.1016/j.matdes.2017.07.067
76. Tazegul O, Dylmishi V, Cimenoglu H (2016) Copper matrix composite coatings produced by cold spraying process for electrical applications. Arch Civil Mech Eng 16(3):344–350. https://doi.org/10.1016/j.acme.2016.01.005
77. Daroonparvar M, Yajid MAM, Kay CM, Bakhsheshi-Rad H, Gupta RK, Yusof NM, Ghandvar H, Arshad A, Zulkifli ISM (2018) Effects of Al2O3 diffusion barrier layer (including Y-containing small oxide precipitates) and nanostructured YSZ top coat on the oxidation behavior of HVOF NiCoCrAlTaY/APS YSZ coatings at 1100 degrees C. Corros Sci 144:13–34. https://doi.org/10.1016/j.corsci.2018.07.013
78. Huang C, Yang K, Li N, Li W, Planche M, Verdy C, Liao H, Montavon G (2018) Microstructures and wear-corrosion performance of vacuum plasma sprayed and cold gas dynamic sprayed Muntz alloy coatings. Surf Coat Technol
79. Yin S, Ekoi EJ, Lupton TL, Dowling DP, Lupoi R (2017) Cold spraying of WC-Co-Ni coatings using porous WC-17Co powders: formation mechanism, microstructure characterization and tribological performance. Mater Des 126:305–313. https://doi.org/10.1016/j.matdes.2017.04.040
80. Watson TJ, Nardi A, Ernst AT, Cernatescu I, Bedard BA, Aindow M (2017) Cold spray deposition of an icosahedral-phase-strengthened aluminum alloy coating. Surf Coat Technol 324:57–63. https://doi.org/10.1016/j.surfcoat.2017.05.049